Environmental Science and Ecotechnology 12 (2022) 100198

Contents lists available at ScienceDirect

Environmental Science and Ecotechnology

journal homepage: www.journals.elsevier.com/environmental-science-and-ecotechnology/

Original Research

# Organophosphate esters cause thyroid dysfunction via multiple signaling pathways in zebrafish brain

Zhenfei Yan [a, b], Chenglian Feng [a, *], Xiaowei Jin [c, **], Fangkun Wang [d], Cong Liu [d], Na Li [e], Yu Qiao [a], Yingchen Bai [a], Fengchang Wu [a, b], John P. Giesy [f, g, h]

[a] State Key Laboratory of Environmental Criteria and Risk Assessment, Chinese Research Academy of Environmental Sciences, Beijing, 100012, China
[b] College of Environment, Hohai University, Nanjing, 210098, China
[c] China National Environmental Monitoring Centre, Beijing, 100012, China
[d] Department of Preventive Veterinary Medicine, College of Veterinary Medicine, Shandong Agricultural University, Taian, 271018, China
[e] Key Laboratory of Drinking Water Science and Technology, Research Center for Eco-Environmental Sciences, Chinese Academy of Sciences, Beijing, 100085, China
[f] Department of Veterinary Biomedical Sciences, University of Saskatchewan, Saskatoon, SK, Canada
[g] Toxicology Centre, University of Saskatchewan, Saskatoon, SK, Canada
[h] Department of Environmental Sciences, Baylor University, Waco, TX, USA

ARTICLE INFO

*Article history:*
Received 21 March 2022
Received in revised form
1 June 2022
Accepted 1 June 2022

*Keywords:*
Organophosphate ester
Molecular docking simulation
Competitive inhibition assay
Thyroid endocrine function
Transcriptome sequencing

ABSTRACT

Organophosphate esters (OPEs) are widespread in various environmental media, and can disrupt thyroid endocrine signaling pathways. Mechanisms by which OPEs disrupt thyroid hormone (TH) signal transduction are not fully understood. Here, we present in vivo-in vitro-in silico evidence establishing OPEs as environmental THs competitively entering the brain to inhibit growth of zebrafish via multiple signaling pathways. OPEs can bind to transthyretin (TTR) and thyroxine-binding globulin, thereby affecting the transport of TH in the blood, and to the brain by TTR through the blood–brain barrier. When GH3 cells were exposed to OPEs, cell proliferation was significantly inhibited given that OPEs are competitive inhibitors of TH. Cresyl diphenyl phosphate was shown to be an effective antagonist of TH. Chronic exposure to OPEs significantly inhibited the growth of zebrafish by interfering with thyroperoxidase and thyroglobulin to inhibit TH synthesis. Based on comparisons of modulations of gene expression with the Gene Ontology and Kyoto Encyclopedia of Genes and Genomes databases, signaling pathways related to thyroid endocrine functions, such as receptor–ligand binding and regulation of hormone levels, were identified as being affected by exposure to OPEs. Effects were also associated with the biosynthesis and metabolism of lipids, and neuroactive ligand–receptor interactions. These findings provide a comprehensive understanding of the mechanisms by which OPEs disrupt thyroid pathways in zebrafish.


*Abbreviations:* AChE, acetylcholinesterase; ANOVA, analysis of variance; BCF, bioconcentration factor; BFR, brominated flame retardant; CD-FBS, charcoal-dextran-treated fetal bovine serum; CDP, cresyl diphenyl phosphate; *cga*, glycoprotein hormone; DEG, differentially expressed gene; DKA, β-diketone antibiotic; DMSO, dimethyl sulfoxide; EAS, estrogen; androgen, and steroidogenesis; FBS, fetal bovine serum; GAPDH, glyceraldehyde-3-phosphate dehydrogenase; GO, Gene Ontology; HPLC-MS/MS, high-performance liquid chromatograph interfaced with a mass spectrometer; HPT, hypothalamic–pituitary–thyroid; HS, horse serum; KEGG, Kyoto Encyclopedia of Genes and Genomes; MAPK, mitogen-activated protein kinase; NIS, $Na^+/I^-$ symporter; $OD_{490}$, optical density; OPFR, organophosphate flame retardant; OPE, organophosphate ester; PBDE, polybrominated diphenyl ether; PBS, phosphate-buffered saline; P/S, penicillin–streptomycin; qRT-PCR, quantitative real-time PCR; $RIC_{20/50}$, concentration inhibiting 20%/50%; T4, thyroxin; TBG, thyroxine-binding globulin; TCIPP, tris(2-chloroisopropyl) phosphate; TDCIPP, tris(1,3-dichloro-2-propyl) phosphate (TDCIPP); TDCIPP-d15, tris(1,3-dichloroisopropyl) phosphate-D15; TG, thyroglobulin; TH, thyroid hormone; THR, thyroid hormone receptor; TIPP, tris(isopropyl) phosphate; TPHP, triphenyl phosphate; TPO, thyroperoxidase; TRβ, thyroid hormone receptor β; tshβa, thyroid-stimulating hormone beta subunit a; TTR, transthyretin.

* Corresponding author.
** Corresponding author.
*E-mail addresses:* fengcl@craes.org.cn (C. Feng), jinxw@cnemc.cn (X. Jin).

https://doi.org/10.1016/j.ese.2022.100198

## 1. Introduction

Because fires can cause significant loss of life and damage to property globally, the inclusion of flame retardants in various potentially flammable products is required in many jurisdictions [1]. Owing to the phasing out and regulation of brominated flame retardants (BFRs), in recent years organophosphate flame retardants (OPFRs) have instead been widely used worldwide as replacements [2,3]. It has been reported that the annual consumption of OPFRs has increased significantly over the last few decades [4,5]. In China, the production of OPFRs has increased at an average, annual rate of 15% [6]. In the U.S.A., it was projected that approximately 50,000 tons of OPFRs would be manufactured per year by 2020 [7]. Because they are often not covalently bound into materials, organophosphate esters (OPEs) can be released into the environment, resulting in their widespread detection in multiple environmental media, including abiotic and biotic compartments [6,8–13] and [14]. OPEs have also been reported to be prone to long-range atmospheric transport away from their sources and can move toward the poles via the "grasshopper effect," which is caused by differential cooling [15,16]. This behavior, eventually results in the global contamination of remote and oceanic environments far from industrial and urban areas where OPEs are manufactured and used [15–18]. Due to this transport in the environment, there is a need for study of the potential exposure of wildlife and humans to OPEs and associated adverse effects.

Recently, multiple mechanisms behind the toxicity of OPEs to aquatic organisms have been reviewed and discussed [19]. Conclusions of that review indicated that neurotoxicity, cardiotoxicity, hepatotoxicity, endocrine disruption including of sex hormones and thyroid hormone (TH), and adverse effects on reproduction and development have been observed, both *in vitro* and *in vivo* [20–25]. Previous results suggested that, in theory, some new chemicals should cause less acute toxicity, but might be more toxic owing to chronic exposure [26]. Furthermore, exposure to OPEs was predicted to disrupt endocrine pathways at environmentally relevant concentrations, which were lower than those causing other toxic effects [27] and [19, 28–32]. Disruption of endocrine functions was also found to be related to changes in the fitness of fish populations [33–35]. Generally, decreases in biodiversity are preceded by changes at the molecular and physiological levels of organization, which result in changes in the functions of tissues and organs, followed by integrative effects on traits such as scope for growth and reproduction, which can be measured based on body mass and length [36]. TH is associated with regulation of the growth of organisms [37] and understanding the mechanisms and adverse outcome pathways of TH can thus be critical to predicting changes in populations [38,39]. Compared with toxicity with direct links to the estrogen, androgen, and steroidogenesis (EAS) modalities, information on the indirect effects of OPEs on the hypothalamic–pituitary–thyroid (HPT) axis of fish and subsequent effects on reproduction remains limited.

In fish, the thyroid modality of toxic action can involve the disruption of multiple targets of thyroid signals and functions along the thyroid hormone-mediated, signal transduction cascade [19,40–42]. Results of recent studies have demonstrated that tris(2-chloroisopropyl) phosphate (TCIPP) can function as an antagonist by inhibiting the binding of 17β-estradiol to estrogen receptor [27], but also reduce functioning of the thyroid gland and increase the activities of hepatic T4-outer ring deiodinase enzymes [22]. When zebrafish embryos/larvae were exposed to tris(1,3-dichloro-2-propyl) phosphate (TDCIPP) and triphenyl phosphate (TPHP), the synthesis of TH via enzymes (*tshβ*, *slc5a5*, and *tg*), metabolism (*dio1*), transport (*ttr*), elimination (*ugt1ab*), and thyroid development (*hhex*, *nkx2.1*, and *pax8*) were affected, which could disrupt central regulation through signaling pathways and synthesis to increase the TH levels in blood plasma [25,29,37]. Aryl, alkyl, and chlorinated OPEs were all considered as potential disruptors of TH and antagonists of thyroid hormone receptor β (TRβ) [43]. However, research into the acute toxicity of OPEs to zebrafish embryos/larvae suggested that aryl OPEs, including cresyl diphenyl phosphate (CDP) and TPHP, were more likely to cause heart malformations, pericardial edema, and cardiac-looping blocking than alkyl and chlorinated OPEs, which was mainly attributed to their hydrophobicity and potential bioaccumulation [21]. Moreover, TPHP has been suggested to be an effective inhibitor of acetylcholinesterase (AChE) activity to induce developmental neurotoxicity in zebrafish [44,45]. To date, research has focused on the mechanisms by which OPEs impact TH by affecting the amounts of hormones produced, while information on the effects on the molecular mechanisms and signaling pathways of TH has remained limited. Thus, an important aspect to be considered is whether there is a specific biomarker, such as a target protein, target molecule, or specific OPE, for the effects of OPEs on thyroid function.

In this study, three typical OPEs were selected to explore the disruption of TH endocrine functions *in vivo*/*in vitro* using zebrafish and GH3 cells, and *in silico* using molecular docking. Results from the combination of these methods elucidated the primary molecular mechanisms at the molecular, gene expression, cell, protein, and individual levels. Modes of transport of OPEs in the blood were also investigated using molecular docking simulation. In addition, GH3 cell assays were used to explore how OPEs competitively enter cells. To elucidate the primary molecular mechanisms behind the disruption of TH-signaling pathways, after chronic exposure, the expression of key genes, hormones, and proteins in target organs was investigated. Specific aims in this study were to: (1) investigate the correlations between TH biosynthesis and OPE transportation *in vivo* with precursor proteins or transporters; (2) discuss molecular modes of action regarding TH endocrine disruption by OPEs; and (3) identify a specific biomarker for the disruption of thyroid function in zebrafish.

## 2. Materials and methods

### 2.1. Chemicals and reagents

Tris(isopropyl) phosphate (TIPP) (CAS 513-02-0), CDP (CAS 26444-49-5), TCIPP (CAS 13674-84-5), and dimethyl sulfoxide (DMSO) were purchased from J&K Scientific, Ltd. (Beijing, China). The internal standard [tris(1,3-dichloroisopropyl) phosphate-D15, TDCIPP-d15] and phosphate-buffered saline (PBS) were purchased from Toronto Research Chemicals, Inc. (Toronto, ON, Canada), and Coolaber (Beijing, China), respectively. All organic solvents were of HPLC-grade purity and were obtained from Thermo Fisher Scientific (Waltham, MA, USA). RPMI-1640 culture medium was purchased from Procell Life Science & Technology Co., Ltd. (Wuhan, China). Charcoal-dextran-treated fetal bovine serum (CD-FBS) and DMEM/F-12 were obtained from HyClone (Logan, UT, USA). MTS kit used for measuring cell proliferation was purchased from Bestbio (Shanghai, China).

### 2.2. Maintenance of zebrafish and exposure to OPEs

Zebrafish were maintained in continuous-flow tanks filled with carbon-filtered water under a photoperiod of 16:8 h light/dark for 25 ± 2 °C. After acclimation, 1-month-old zebrafish were exposed to TIPP, CDP, or TCIPP following OECD test guidelines protocol no. 229 with minor modifications (*OECD 229*). Briefly, zebrafish were exposed individually in a semi-static exposure system to 10, 50, or 100 μg $L^{-1}$ of each OPE or blank control for 28 days. A carrier of

0.01% DMSO (v/v) was used and exposure was performed in triplicate. Fifteen zebrafish were exposed in 3 L of dechlorinated carbon-filtered water filtered via a 0.45 μm filter membrane. During 28 dexposure, half of the exposure solution was replaced daily with freshly prepared filtered water, containing a corresponding concentration of TIPP, CDP, or TCIPP. Exposure solutions were sampled before and after renewing these solutions, 4 mL of which were filtered via a 0.45 μm Minisart syringe filter (Sartorius, Göttingen, Germany), followed by storage at −20 °C until analysis. Detailed protocols used for the identification and quantification of TIPP, TCIPP, and CDP in exposure solutions and biota are provided in the Supporting Information (SI) (Tables S1 and S2 and Fig. S1), using a high-performance liquid chromatograph interfaced with a mass spectrometer (HPLC-MS/MS, Nexera-X2/8040; Shimadzu Co. Ltd., Kyoto, Japan) with a Waters C18 column (50 mm × 2.1 mm, 3.5 mm). The mass and snout-to-vent length of each zebrafish were measured before and after the exposure. Blood was collected from the caudal vein using glass capillary tubes to quantify thyroxin (T4). Brain and soma samples were collected for the quantification of T4, thyroperoxidase (TPO), and thyroglobulin (TG). Transcriptome sequencing analysis was performed and the protein levels of thyroxine-binding globulin (TBG), transthyretin (TTR), and $Na^+/I^-$ symporter (NIS) were quantified. Detailed protocols are provided in the Supporting Information Section SIV.

### 2.3. Competitive inhibition assay and Western blot on GH3 cell lines

Rat pituitary tumor GH3 cells were purchased from Procell Life Science & Technology Co., Ltd. (Wuhan, China), and cultured in Ham's F−12K culture medium supplemented with 15% horse serum (HS), 2.5% fetal bovine serum (FBS), and 1% penicillin−streptomycin (P/S) at 37 °C in a humidified atmosphere with 5% $CO_2$. Cells were stored in liquid nitrogen with cell freezing medium containing 55% basic medium, 40% FBS, and 5% DMSO.

Based on the proliferation of GH3 cells for 96 h, the concentrations of OPEs and T4 that caused 20% ($RIC_{20}$) or 50% ($RIC_{50}$) inhibition of cell proliferation were calculated (Table S3). Proliferation of cells in the T-screen assay for 96 h was carried out by slightly modified versions of previously published methods [43,46,47]. Briefly, cells were cultured for 48 h in phenol red-free, RPMI-1640 culture medium with 5% CD-FBS, and 1% P/S. Cells were collected from culture plates and used in the competitive inhibition assay conducted in a transparent 48-well culture plate. The experimental design included a blank control (0.1% v:v DMSO); exposure to T4, CDP, TIPP, or TCIPP individually; or exposure to combinations of T4 and OPEs: T4+CDP, T4+TIPP, or T4+TCIPP. Concentrations administered for the exposure were set to either $RIC_{20}$ or $RIC_{50}$. Each exposure solution was conducted in triplicate and refreshed every 24 h during 96 h of exposure. Absorption measured as optical density ($OD_{490}$), which was used as a measure of cell proliferation, was determined via a microplate reader at 490 nm after treatment with the MTS kit [43]. The remaining cells were subjected to western blotting to determine the levels of proteins of TBG, TTR, and NIS, with the results normalized to glyceraldehyde-3-phosphate dehydrogenase (GAPDH) expression. The detailed procedure is provided in Supporting Information Section SIII.

### 2.4. Transcriptome sequencing (RNA-seq) in zebrafish brain

Brain samples were taken from each control or treatment group after 28 d. Six brain samples were taken from each replicate exposure and used for transcriptome sequencing related to key signaling and functional processes of the HPT axis. An RNA-seq transcriptome library was prepared by extracting total RNA in TRIzol® Reagent, using the TruSeq™ RNA sample preparation kit from Illumina (San Diego, CA, USA). Before read mapping for these samples, a paired-end RNA-seq sequencing library was sequenced with the Illumina HiSeq xten/NovaSeq 6000 sequencer (2 × 150 bp read length). Differentially expressed genes (DEGs) were analyzed by RSEM (http://deweylab.biostat.wisc.edu/rsem/). Functional enrichments with the Gene Ontology (GO) and Kyoto Encyclopedia of Genes and Genomes (KEGG) databases were carried out using Goatools (https://github.com/tanghaibao/Goatools) and KOBAS (http://kobas.cbi.pku.edu.cn/home.do). Detailed protocols used for the RNA-seq of TIPP, TCIPP, and CDP are provided in Supporting Information Section SV. To validate the results of transcriptome analysis, several DEGs calculated by RSEM were selected to conduct the quantitative real-time PCR (qRT-PCR) for the brain samples, as detailed in Supporting Information Section SVI.

### 2.5. Molecular docking simulation

The structures for OPEs and T4 investigated in this study were built and optimized using the software package Discovery Studio Visualizer 4.0 (DS4.0; Accelrys Inc., CA, USA). Molecular docking with TBG (ID: 2RIW) and TTR (ID: 1ICT 3.0 Å) were obtained from the Protein Data Bank (PDB, www.rcsb.org). The molecular docking was performed with the cdocker protocol in DS4.0 based on the results of previous research [48,49]. During the molecular docking, at least 20 random ligand conformations generated in this study were further refined by grid-based simulated annealing in the binding site. Final interaction energy was selected from top-ranking poses derived during the docking analysis.

### 2.6. Statistical analyses

All statistical analyses in this study were performed using IBM SPSS Statistics 22.0 (IBM Corporation, Armonk, NY, USA) and Origin 2018 (OriginLab Corporation, Northampton, MA, USA). First, the normality of parameters was checked using the Shapiro−Wilks test, and the assumption of homogeneity of variance was evaluated using Levene's test. One-way analysis of variance (ANOVA) with least significant difference was used as a multiple range test to measure the significance of differences between the control and OPE-treated groups. The results from at least three independent repetitions were expressed as mean ± standard deviation (SD). In this study, significant differences between the control and treatment groups were defined by a $p$-value less than 0.05.

## 3. Results

### 3.1. Analysis of growth inhibition in zebrafish induced by OPEs

Exposure of zebrafish to TIPP, CDP, or TCIPP inhibited growth and development as determined by body mass and length measurements (Fig. 1a). Exposure to 10 μg CDP $L^{-1}$ resulted in significantly shorter body length, whereas exposure to other concentrations of CDP did not have significant effects. There was no significant change of body mass in zebrafish exposed to CDP. Exposure to 50 μg $L^{-1}$ TIPP or TCIPP significantly decreased the body length of zebrafish compared with that in the control. Exposure of zebrafish to TIPP ranging from 10 to 100 μg $L^{-1}$ resulted in significantly, dose-dependently greater body mass, while for TCIPP, no significant inhibition was observed, except for with 100 μg TCIPP $L^{-1}$. Impacts on body mass were the major effects of TIPP, while exposure to TCIPP affected body length.

The concentrations of CDP in tissues of zebrafish exposed to 10, 50, and 100 μg $L^{-1}$ were dose-dependent and were 5.26 ± 1.90, 21.63 ± 6.42, and 27.43 ± 2.01 ng $g^{-1}$ wet mass (w/w), respectively

(Table S2). Concentrations of TCIPP in tissues of zebrafish were found at 100 μg TCIPP $L^{-1}$, namely, 20.99 ± 7.31 ng $g^{-1}$ w/w. However, upon exposure to TIPP, TIPP was consistently not detected in zebrafish tissues.

### 3.2. Analysis of contents of T4, TG, and TPO in various tissues of zebrafish

Contents of T4, TG, and TPO in blood plasma, brain, and somatic tissues (muscle) were measured by ELISA kits to analyze the correlation between hormone levels and growth of zebrafish after exposure to OPEs for 28 d. Exposure of zebrafish to OPEs for 28 d affected the concentrations of T4 in blood plasma, brain, and somatic tissues (muscle) (Fig. 1b and S4a). No significant changes in the contents of T4 were observed in the brain of zebrafish exposed to TCIPP (Fig. 1b). Compared with controls, exposure to CDP caused significantly, dose-dependent, lower contents of T4 in the brain, while exposure to TIPP caused dose-dependent effects at greater contents of T4 ($p < 0.05$ only at 10 μg $L^{-1}$), which were all less than that of the control. The only exception was 100 μg $L^{-1}$. Exposure to CDP and TIPP caused dose-dependent lower total contents of T4 in the blood plasma (Fig. 1b). Compared with the control, the lower content of T4 in the blood plasma was significant at 100 μg CDP $L^{-1}$, and the greater content was significant at 10 μg TIPP $L^{-1}$. Contents of T4 were significantly lower in zebrafish exposed to 10 μg TCIPP $L^{-1}$, while no significant effects on T4 were observed in zebrafish exposed to other concentrations of TCIPP. Exposure to CDP, TIPP, or TCIPP, except for 50 μg CDP $L^{-1}$ and 100 μg TIPP $L^{-1}$, did not significantly affect the contents of T4 in somatic tissue (Fig. S4a). Ranges of the contents of T4 in the brain and somatic tissue of zebrafish exposed to CDP, TIPP, or TCIPP accounted for 4.2–9.3% and 3.6–9.6% of the total plasma concentrations of T4, respectively. Mean values of the percentages of T4 in the brain and somatic tissues were 6.7 ± 1.2% and 5.9 ± 2.2%, which were less than one-tenth of the total contents of T4 in blood plasma. Contents of T4 in the brain were greater than those in somatic tissue.

Exposure of zebrafish to CDP, TIPP, or TCIPP caused dose-dependent changes in the contents of TPO and TG which are key proteins in the synthesis of TH in the brain (Fig. 1c). Compared with the control, exposure of zebrafish to CDP caused significantly, dose-dependently lower TG in the brain, but significantly, dose-dependently greater contents of TPO upon exposure to 100 μg CDP $L^{-1}$. Zebrafish exposed to TIPP had significantly lower contents of TPO in the brain relative to the controls, while the contents of TG were significantly lower than those of controls in zebrafish exposed to the greatest concentration (100 μg TIPP $L^{-1}$). During chronic exposure to TCIPP, contents of TG in the brain increased in a dose-dependent manner, and that upon exposure to the greatest concentration (100 μg TCIPP $L^{-1}$) was significantly increased. Contents of TPO in the brain were lower than those of the controls in zebrafish exposed to TCIPP. For somatic tissue (muscle), contents of TG in fish exposed to CDP or TIPP were greater than those in controls in a dose-dependent manner (Fig. S4b). Contents of TPO upon exposure to CDP were reduced in a dose-dependent manner, while they increased in a dose-dependent manner in zebrafish exposed to TIPP (Fig. S4b).

### 3.3. Transcriptome analysis of thyroid disruption caused by OPEs in brain

RNA-seq was used to investigate the key signaling pathways of thyroid dysfunction induced by OPEs in zebrafish. According to the hierarchical cluster analysis of 91 thyroid-related genes or 35 co-expressed genes related to thyroid function, the patterns of expression of genes in fish exposed to TIPP or TCIPP were similar, which differed from the pattern in the brain of fish exposed to CDP (Figs. S9 and S10). The patterns of expression of all genes in un-exposed controls also differed from those of fish exposed to OPEs. Twenty-four DEGs related to thyroid function were selected from 9793 DEGs in all samples, which were annotated for the *Danio rerio* genome, and used for hierarchical cluster analysis and functional enrichment analyses of both GO databases (Figs. 2 and 3, Tables S20 and S21). The results of the functional annotation analysis for thyroid-related genes identified certain GO terms, with the genes being particularly involved in biological processes (e.g., cellular process and biological regulation), cellular components (e.g., cell parts and organelle), and molecular functions (e.g., binding) in zebrafish (Fig. 3a, S11a, and S12a). Based on classified statistics of KEGG signaling pathway, environmental information processing pathways (e.g., signaling molecules and interaction, and signal transduction) were the main KEGG pathways related to the effects of nerve conduction on the thyroid (Figs. S11c and S12c). The results of functional enrichment analyses, using GO and KEGG, demonstrated significant changes of multiple signal pathways related to thyroid effects among all OPE treatments, including binding to TH receptor (THR), thyroid hormone generation, thyroid hormone metabolic process, thyroid hormone transmembrane transporter activity, thyroid gland development, neuroactive ligand–receptor interaction, and insulin signaling pathway ($p$-adjust ≤ 0.05) (Fig. 3b, S11b and d, and S12b and d, Table S6). Regulation of lipid biosynthetic process ($p$-adjust < 0.05) could be induced by thyroid-related genes after exposure to OPEs (Fig. 3b, S11b, S12b, and S13). Thyroxine 5′-deiodinase activity, which plays an important role in thyroid hormone generation, was also significantly enriched in the GO analysis ($p$-adjust <0.05) (Figs. S11b and S12b). Based on the correlation analysis of gene and protein interactions (Figs. S13 and S14), disruption of thyroid function by OPEs might be associated with certain signaling pathways related to the nervous system and lipid biosynthesis.

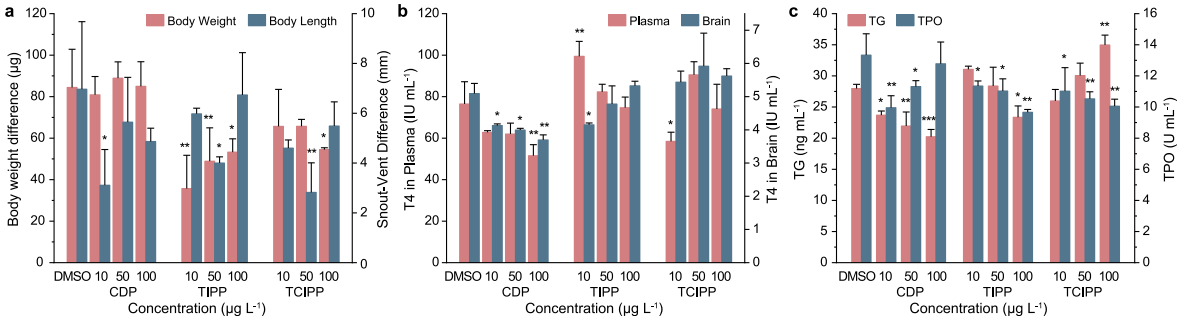


**Fig. 1.** Inhibition of growth and hormone imbalance of zebrafish exposed to CDP, TIPP, or TCIPP for 28 d **a**, Body mass and length of zebrafish exposed to OPEs. **b**, Concentrations of T4 in blood plasma or brain after 28 d exposure. **c**, Concentrations of TG and TPO in brain of zebrafish. Mean ± standard deviation (SD, n = 3), *$p < 0.05$, **$p < 0.01$, ***$p < 0.001$.

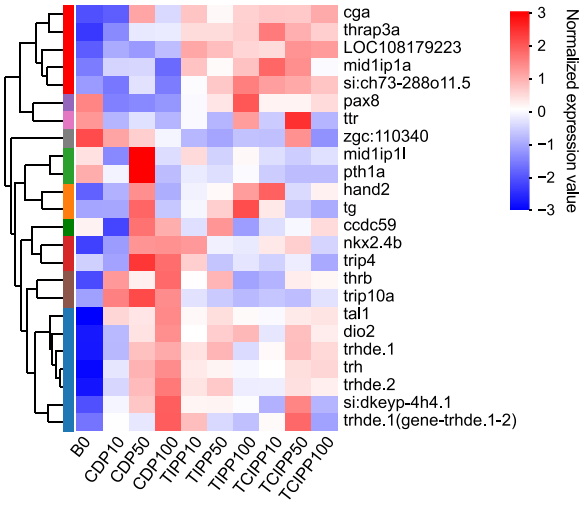


**Fig. 2.** Hierarchical clustering analysis of DEGs related to thyroid effects (24 genes) selected from 9793 DEGs in all samples exposed to CDP, TIPP, and TCIPP in zebrafish brain. Colors in the figure indicate normalized expression of genes in each sample. Red represents overexpression of genes and blue represents under-expression. To the left is a tree diagram of gene clustering and the module diagram of sub-clustering, and to the right is the names of genes. The names of the samples are shown at the bottom.

### 3.4. Quantitative analysis of TBG, TTR, and NIS levels based on RNA-seq results

To verify that transmembrane transport and blood transportation are key signaling pathways, as determined by transcriptional analysis, TTR, TBG, and NIS in the brain were measured by ELISA. Compared with the levels in the control, concentrations of TTR in fish exposed to CDP increased in a dose-dependent manner (Fig. 4a). Exposure to 50 or 100 μg CDP $L^{-1}$ resulted in significantly greater concentrations of TTR. Exposure to TIPP or TCIPP resulted in significantly ($p < 0.01$) greater concentrations of TTR in the brain after 28-d exposure. Concentrations of TBG in the brain were not significantly altered by exposure to CDP, TIPP, or TCIPP compared with those of the unexposed control (Fig. 4b). Concentrations of NIS in the brain were generally greater in individuals exposed to CDP, TIPP, or TCIPP than those in brains of unexposed controls (Fig. 4c), especially exposure to 10 or 50 μg CDP $L^{-1}$, 100 μg TIPP $L^{-1}$, and all concentrations of TCIPP.

### 3.5. Competitive inhibition and Western blot analysis of T4 or OPEs

To explore the effects of OPEs on cell proliferation, a competitive inhibition assay was performed on GH3 cells. Based on acute toxicity, exposure to T4 promoted the proliferation of cells, while exposure to OPEs inhibited such proliferation (Table S3). Upon analysis of competitive correlations among OPEs and T4 based on colorimetric responses of the MTS kit (Fig. 5), with $RIC_{20}$ as the endpoint, $OD_{490}$ values for cells exposed to individual OPEs were not significantly different from those of cells exposed simultaneously to OPEs in the presence of T4 (T4+OPEs). $OD_{490}$ values upon exposure to T4 individually were significantly greater than those of T4+OPEs ($p < 0.01$). However, when the endpoint was the $RIC_{50}$, exposure to T4+CDP resulted in significantly greater proliferation of GH3 cells than exposure to either T4 or CDP alone ($p < 0.01$). Exposure to T4+TIPP can significantly inhibit the proliferation of GH3 cells compared with that of cells exposed to T4 or TIPP alone ($p < 0.01$). Simultaneously, exposure to T4+TCIPP resulted in significantly greater proliferation than exposure to

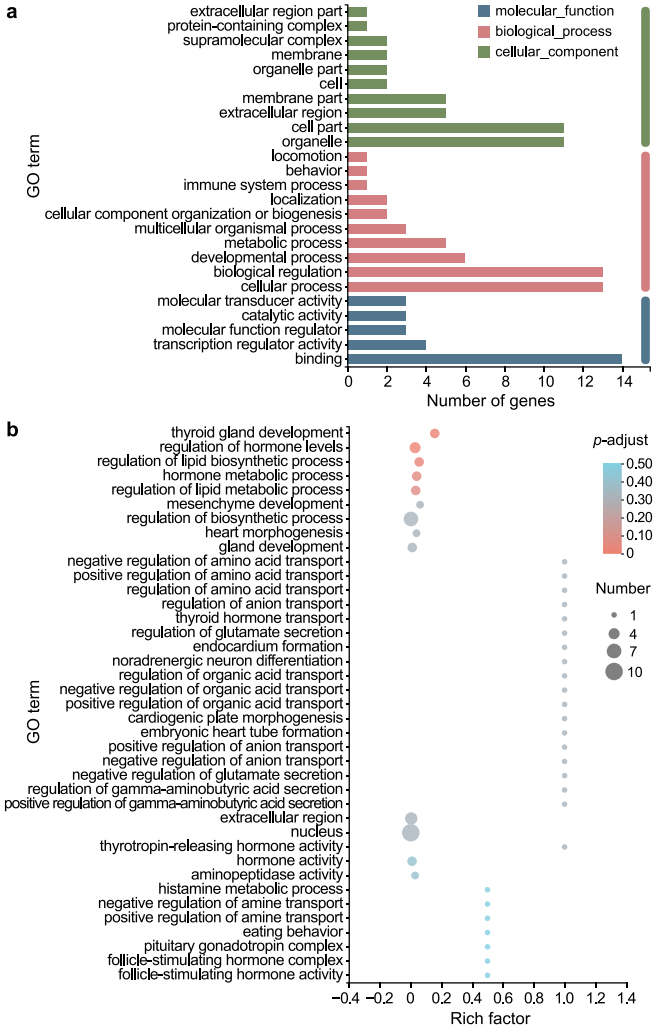


**Fig. 3.** Functional enrichment analysis of DEGs related to thyroid effects (24 genes) in samples exposed to CDP, TIPP, or TCIPP. **a**, Functional annotation analysis based on the GO database of 24 DEGs related to thyroid effects in all brain samples exposed to CDP, TIPP, or TCIPP. **b**, Top 39 GO terms of enrichment from the GO database of DEGs ($p$-adjust < 0.5). Enrichment factor represents the ratio of the number of genes enriched in the GO term and the total number of annotated genes. Size of dots indicates the numbers of genes associated with the GO term, while colors of dots correspond to $p$-adjusted ranges.

TCIPP alone ($p < 0.05$), while it resulted in significantly less proliferation than that by cells exposed solely to T4 ($p < 0.001$). In addition, expression of TTR protein was not detected in GH3 cells (Fig. S2). This might have been due to the occurrence and distribution of TTR protein in cells. In the case of the $RIC_{20}$, compared with GH3 cells exposed to T4 alone and blank control, concentrations of NIS were significantly decreased upon exposure to TIPP, TCIPP, or T4+OPEs, while there was no significant difference at the $RIC_{50}$. Likewise, at the $RIC_{50}$, there was significantly more TBG in GH3 cells exposed to TIPP, TCIPP, and OPEs with T4, compared with cells exposed to T4 alone, while there were no significant differences at the $RIC_{20}$.

### 3.6. Analysis of interaction of OPEs with TBG and TTR

Based on the molecular docking simulation, the interactions between OPEs and TBG or TTR were analyzed and compared with

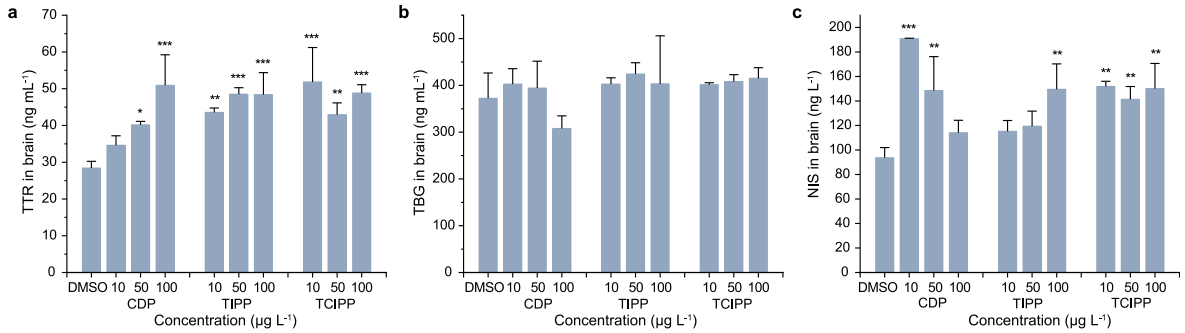


**Fig. 4.** Amounts of TTR, TBG, and NIS proteins in brain after 28 d of exposure of zebrafish to CDP, TIPP, or TCIPP. **a**, Changes in concentrations of TTR in the brain of zebrafish exposed to CDP, TIPP, or TCIPP. **b**, Changes in concentrations of TBG in brain. **c**, Changes in concentrations of NIS in brain. Mean ± standard deviation (SD, n = 3), *$p < 0.05$, **$p < 0.01$, ***$p < 0.001$.

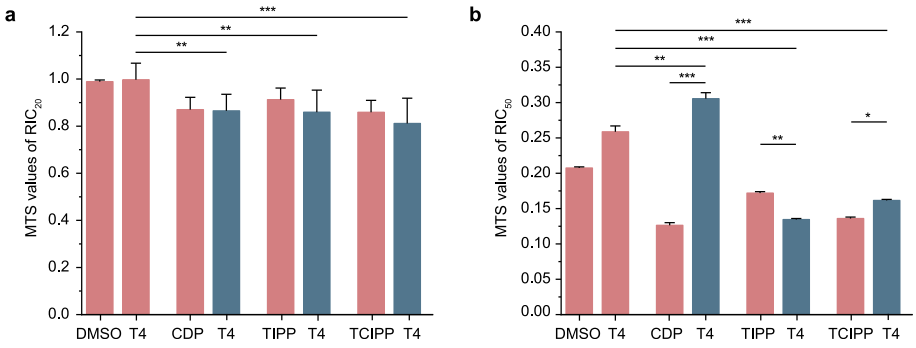


**Fig. 5.** Proliferation of GH3 cells assessed using the MTS kit after exposure to the $RIC_{20}$ and $RIC_{50}$ of CDP, TIPP, and TCIPP for 96 h **a**, Changes in the proliferation of GH3 cells exposed to $RIC_{20}$. **b**, Changes in the proliferation of GH3 cells exposed to $RIC_{50}$. Mean ± standard deviation (SD, n = 3), *$p < 0.05$, **$p < 0.01$, ***$p < 0.001$.

**Table 1**
The binding affinity of OPEs for TBG and TTR using molecular docking.

| Chemicals | CAS | TBG | | TTR | |
|---|---|---|---|---|---|
| | | Cdocker Energy kcal $mol^{-1}$ | Interaction | Cdocker Energy kcal $mol^{-1}$ | Interaction |
| T4 | 300-30-1 | −47.0479 | ASN A: 273[a], ARG B: 381 [b] | −42.6893 | SER B: 117[a], SER D: 117[a], LYS D: 15[a] |
| TIPP | 513-02-0 | −48.634 | — | −50.7945 | — |
| CDP | 26444-49-5 | −38.183 | ARG B: 381 [b], LYS A: 270 [b] | −40.128 | LYS B: 15 [b] |
| TCIPP | 13674-84-5 | −54.5853 | — | −55.6138 | LYS D: 15[a] |
| TNBP | 126-73-8 | −60.4225 | — | −57.6073 | — |
| TPHP | 115-86-6 | −34.1994 | ARG B: 381 [b] | −36.3499 | LYS B: 15 [b] |
| TDCIPP | 13674-87-8 | −56.755 | — | −53.7351 | LYS D: 15[a] |

**Note:** a: Hydrogen bond interaction; b: π−cation interaction; —: There is no amino acid binding site between OPEs and TBG or TTR, while van der Waals interaction and hydrophobic interaction mainly occur.

the interactions between T4 and TBG or TTR. Amino acid binding sites involved in the interaction between OPEs or T4 and TBG were Asn A 273, Arg B 381, and Lys A 270, while those involved in interactions between OPEs or T4 and TTR were Ser B 117, Ser D 117, Lys D 15, and Lys B 15 (Table 1, Figs. S16 and S17). Based on "cdocker" energy, binding affinities of OPEs to TBG were in the following order, TNBP > TDCIPP > TCIPP > TIPP > T4 > CDP > TPHP, while those to TTR were TNBP > TCIPP > TDCIPP > TIPP > T4 > CDP > TPHP (Table 1). Affinities of binding between TIPP or TCIPP and TBG or TTR were greater than those of T4 and CDP. When interacting with TBG, Arg B 381 was the common amino acid binding site of T4 or aryl-OPEs (CDP and TPHP), while Asn A 273 and Lys A 270 were specific ones of T4 and CDP, respectively. In addition, Lys D 15 was the common amino acid binding site of T4 or TCIPP interacting with TTR. However, Lys B 15 was the specific amino acid binding site for CDP and TPHP when interacting with TTR, and Ser B 117 and Ser D 117 were the only binding sites for interaction between T4 and TTR. Chlorinated OPEs might interact with TBG via van der Waals or hydrophobic interaction, while alkyl OPEs might interact with TBG and TTR via van der Waals or hydrophobic interaction.

## 4. Discussion

Disruption of the TH hormone function by exogenous substances that adversely affect the HPT axis can play significant roles in vertebrate development and homeostasis related to growth and energy metabolism [50,51]. In this study, when 1-month-old zebrafish were chronically exposed to OPEs for 28 d, thyroid function was disrupted at the molecular level (*in silico*), and concentrations of hormones, transcription of RNA, and concentrations of proteins were altered *in vivo* and *in vitro*, which resulted in the inhibition of zebrafish growth.

### 4.1. Significant accumulation of CDP rather than TIPP and TCIPP in zebrafish

A growing number of studies have validated that the three OPEs are present in fish as well as in ambient surface water [14, 32, 52]. In the present study, the differential distribution of concentrations of OPEs in tissues of zebrafish was identified and suggested to be due to the greater hydrophobicity and greater bioconcentration factor (BCF) of CDP than those of TIPP and TCIPP. These results were consistent with the following: (1) During long-term exposure, the accumulation of OPEs in aquatic organisms was proportional to the concentrations to which they were exposed. (2) Greater bioconcentrations of CDP in tissues of zebrafish were observed, while there was little bioconcentration of TIPP in such tissues. In fact, in contrast to alkyl OPEs and chlorinated OPEs, TPHP was generally detected in three different tissues of Chinese rare minnow and was found at greater concentrations in male gonad and liver [52]. Based on these results and those of previous studies, differences in toxic potencies caused by the same concentrations of OPEs might be related to differences in detection methods, exposure environments, and pathways of exposure [19,53]. Thus, internal doses, as determined by the concentrations accumulated in tissues of aquatic organisms among exposure media, might better reflect bioavailability and the actual concentration of toxicity effects than the traditional measure of exposure dose, namely, the nominal ambient concentration. Briefly, the concentrations of CDP accumulated in tissues of zebrafish were greater than those of other OPEs, and CDP also caused observable adverse effects, which supported the hypothesis that the greater potency of CDP was due to its greater accumulation.

### 4.2. OPEs regarded as environmental hormones with TH effect in zebrafish

TPO is the primary enzyme involved in the synthesis of TH, while TG is the prohormone and storage form of TH; both are markers of the physiological function of the thyroid gland [54]. Thus, changes in the content of T4 are closely related to the contents of the two proteins TPO and TG. Exposure to environmentally relevant concentrations of CDP, TIPP, or TCIPP was shown to result in changes in the concentrations of T4 in blood plasma, brain, and somatic tissue, as well as changes in the amounts of TPO and TG in brain and muscle. Results of previous studies demonstrated that the exposure of American kestrels (*Falco sparverius*) to environmentally relevant concentrations of OPEs for 21 d might decrease thyroid gland activity and increase hepatic deiodinase activity, eventually influencing concentrations of free T4 or T3 in blood plasma [22]. The results of another study demonstrated that exposure to TPHP can disrupt central regulation and pathways of synthesis, metabolism, transport, and elimination of TH, thus increasing the concentrations of TH in embryos/larvae of zebrafish [37]. It has been reported that OPEs could cause thyroid endocrine disruption of not only adult zebrafish, but also their offspring via the maternal transfer of OPEs [25]. Additionally, in epidemiological studies, TPO and TG have been considered to be key indicator proteins to be monitored to interpret thyroid endocrine disorders [54]. In previous studies of thyroid diseases, thyrotropin receptor, TPO, TG, NIS, and pendrin proteins were identified as antigens that resulted in an autoimmune pathogenic response, which also included molecular mechanisms and signaling pathways associated with thyroid diseases [54–57]. TPO and TG could be identified by CD8-positive T cells, and induce Hashimoto's thyroiditis leading to the destruction of thyroid tissue, which was considered to be a manifestation of clinical disease [58]. Further research has found that TPO and TG are targets of IgE or IgG autoantibodies during chronic, spontaneous urticaria or hypothyroidism [59]. Chronic exposure of zebrafish to OPEs for 1 month resulted in positive correlations between the concentrations of TPO or TG in the brain and the concentrations of T4 in blood plasma, especially upon exposure to CDP. Similarly, the ratio of concentrations of T4 in brain to the total concentration of T4 in blood plasma was greater than that in somatic muscle. These results indicated that exposure to OPEs might affect the concentrations of TPO and TG in the brain, thereby disturbing the synthesis and secretion of TH, whose concentrations were closely related to the development of the brain. Together, this information suggests that the brain plays a vital role in the thyroid endocrine system. The results of several studies have shown that the developing brain tends to be more sensitive to xenobiotics, such as OPEs, and changes in concentrations of TH can significantly affect normal brain development, even adversely affecting the behavior of the offspring of exposed individuals [60,61]. Briefly, the results of the proteins analysis suggested that exposure to OPEs could affect the levels of TPO and TG in brain, resulting in anomalous changes in the concentrations of T4 in blood plasma and brain tissue. This in turn resulted in slower growth of zebrafish owing to lower concentrations of T4 in blood plasma.

### 4.3. Thyroid dysfunction induced by OPEs via multiple signaling pathways including nerve conduction and lipid regulation

Functional enrichment analysis of DEGs by GO and KEGG showed that the effects of growth inhibition of thyroid function in zebrafish were due to interactions with and modulation of multiple signaling pathways. Chronic exposure of zebrafish to OPEs affected significant signaling pathways by altering the binding of TH to the THR, development of the thyroid gland, synthesis and metabolism of TH, thyroid hormone transmembrane transporter activity, and neuroactive ligand–receptor interaction, which eventually resulted in effects on the thyroid in zebrafish that were in the stage of rapid development (Fig. 6 and Table S6). Receptor–ligand binding was the key signaling pathway of the endocrine-disrupting effects induced by chemicals. Therefore, the binding of TH to the THR was considered to be a primary potential target of thyroid disruption induced by OPEs [43]. It was found that OPEs could competitively bind to the membrane THR with TH to enter the cells, inducing thyroid endocrine disruption [49,62]. The results of previous RNA-seq demonstrated that OPEs can affect certain signaling pathways related to the synthesis and metabolism of TH, causing thyroid dysplasia, which resulted in lower concentrations of T4 and caused abnormal development in the early life stages of zebrafish [29,37]. For example, in this study, OPEs could affect the content of T4 through the changes in contents of TPO and TG. It was found that lipid biosynthetic and lipid metabolic processes played important roles in the growth and development of organisms, in which *cga* (encoding a glycoprotein hormone) might be a key gene (Fig. 6 and S13) [63,64]. The results of this study showed that exposure to OPEs can cause significant enrichment of neuroactive ligand–receptor interactions and alter the mitogen-activated protein kinase (MAPK) signaling pathway. Exposure to β-diketone antibiotics (DKAs) caused alterations in 149 KEGG-annotated metabolic pathways in $F_1$ zebrafish, of which the primary affected pathway was the MAPK signaling pathway, followed by neuroactive ligand–receptor interactions [65]. Similarly, exposure of *Daphnia magna* to tributyltin significantly affected the neuroactive ligand–receptor interaction signaling pathways involved in reproduction and development [66]. Previous studies confirmed that thyroid disruption was linked to neurodevelopmental effects [25,61,67]. In brief, the findings suggested that the growth inhibition observed in zebrafish exposed to OPEs might be due to the mode of action of thyroid endocrine disruption, including via neurodevelopment and lipid regulation.

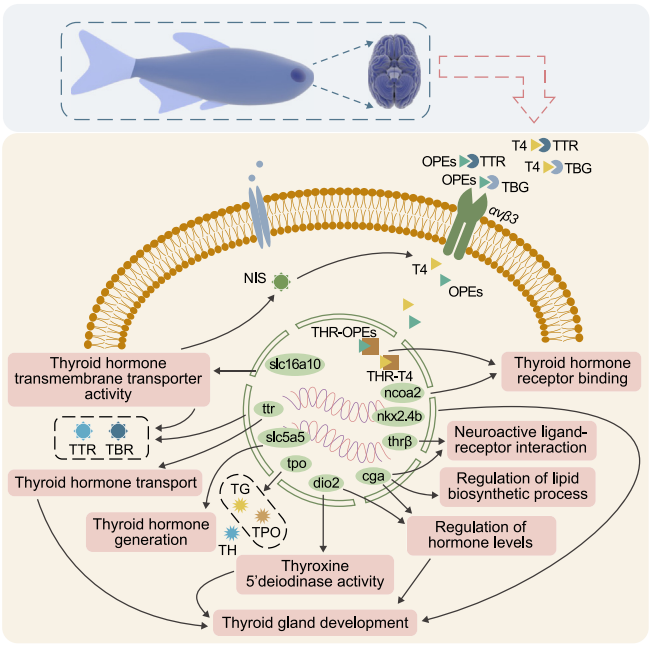


**Fig. 6.** Schematic representation of the speculated mechanisms of toxicity of three OPEs on the disruption of functions of the thyroid axis in zebrafish brain. (Top) Exposure of zebrafish to OPEs affected the brain. (Down) In brain, OPEs competed with T4 to bind to TBG or TTR (especially TTR) for transport, and entered cells through transmembrane proteins affected by NIS. The subsequent interaction of nuclear THR with OPEs or T4 induced abnormal expression of some thyroid-related genes, such as *slc16a10*, *ttr*, *slc5a5*, *tpo*, *dio2*, *cga*, *thrβ*, *nkx2.4b*, and *ncoa2*, which could induce multiple signaling pathways related to thyroid function. For example, the abnormal expression of *tpo* can affect levels of TPO protein in cells, which together with TG caused abnormal changes in TH contents. In addition, expression of *ttr* can affect levels of TTR protein. Due to these signaling pathways, OPEs may cause thyroid dysfunction in zebrafish brain.

### 4.4. TTR is a likely biomarker of thyroid disruption in zebrafish induced by OPEs

As the primary carrier proteins for T4 in blood plasma, TBG and TTR play crucial roles in transporting TH to organs and tissues. NIS mainly expressed in the basolateral membrane of thyroid cells was reported to be important for mediating the transmembrane transport of iodine [68]. In blood plasma, most T4 (70%) was found to bind to TBG with greater affinity than to TTR, to which only 10–15% of T4 bound, yet less than 1% of T4 was present in blood [69,70]. These results suggested that TBG plays a role in binding to and transporting T4 in blood plasma. However, the results involving these proteins in the brain have demonstrated that the concentrations of TTR and NIS were significantly affected by OPEs, but the amounts of TBG were not changed. These findings indicated that TTR was important for the transport of TH or exogenous sources of natural hormones (e.g., OPEs) into the brain of zebrafish. It was also reported that T4 could localize in the brain and cerebrospinal fluid by passing through the blood–brain barrier after combining with TTR [71–73]. Simultaneously, greater amounts of NIS could increase the transmembrane transport activity of iodine, which might subsequently result in greater concentrations of TH [68]. Based on the Western blot results of GH3 cells, rather than TTR and TBG, NIS might play an important role in the generation of T4. In addition, based on the results of transcriptome analysis, TH transmembrane transporter activity might be related to the concentrations of NIS (Fig. 6). However, the changes of T4 in this study were not completely correlated with the concentrations of NIS, which suggested that the concentrations of T4 in zebrafish were affected by multiple factors rather than the intracellular concentrations of iodine (Figs. 1 and 4). Furthermore, the results of molecular docking simulation showed that molecular docking sites of CDP to TBG and TTR were similar to those for T4, while TCIPP would preferentially bind to TTR rather than CDP or T4, and form more stable bonds with TTR than TIPP. The results of several studies have indicated that molecular docking sites of T4 on TBG included hydrogen bond interaction at Asn 273, π–cation interaction at Arg 381, and salt bridge interaction at Lys 270, while those of binding of T4 to TTR involved hydrogen bond interaction with Lys 15 and Ser 117 [70,74,75]. However, the binding of CDP by hydrogen bonding had greater cdocker energy than that of T4, so it decreased the levels of free T4 in plasma or brain tissues. TIPP and TCIPP showed higher binding affinities to TBG and TTR via van der Waals interaction and hydrophobic interaction than those of T4, which increased the levels of free T4 in plasma or brain tissues. It was thus confirmed that TH transmembrane transporter activity and TH transport may be important signaling pathways of thyroid dysfunction induced by OPEs in zebrafish, suggesting that TBG or TTR could transport OPEs in blood plasma and NIS might be the predominant transmembrane protein affecting intracellular TH biosynthesis (Fig. 6). In particular, the combination of OPEs and TTR can be transported to the brain through the blood–brain barrier, thus affecting brain development and altering homeostasis, which suggests that TTR might be a biomarker for thyroid disruption in zebrafish.

### 4.5. GH3 cell proliferation effectively inhibited by OPEs

TH-disrupting chemicals, including BFRs, OPFRs, and polybrominated diphenyl ethers (PBDEs), have been classified as another class of endocrine-disrupting chemicals other than environmental estrogens [37,43,76–80]. Based on results of the T-screen assay and Western blot analysis, the proliferation of GH3 cells was inhibited by OPEs compared with the level in blank control cells or cells exposed only to T4. The inhibitory effects of OPEs obtained using $RIC_{20}$ and $RIC_{50}$ calculated by acute assay of GH3 cells were in the following order: CDP ($RIC_{20}$ = 2.4 nM, $RIC_{50}$ = 0.38 μM) > TCIPP ($RIC_{20}$ = 1.4 μM, $RIC_{50}$ = 90.3 μM) > TIPP ($RIC_{20}$ = 1.4 μM, $RIC_{50}$ = 1.8 mM). The results of Western blot analysis of NIS and TBG in cells exposed to $RIC_{20}$ and $RIC_{50}$ concentrations further confirmed that OPEs, as antagonists, might compete with T4 to inhibit GH3 cell proliferation. It was also found that adverse effects on GH3 cells induced by TIPP and TCIPP co-exposed with T4 at the $RIC_{50}$ were significantly different from those of CDP under the same conditions. T4-TIPP and T4-TCIPP significantly inhibited cell proliferation, while T4-CDP significantly promoted cell proliferation compared with the levels in the blank and T4 groups. The reason for these effects might be the competitive inhibition process of TIPP, TCIPP, or CDP with T4 (Fig. 6), indicating that the superiority of TIPP and TCIPP led to a decrease of the T4 effect, and the inferiority of CDP led to an increase of the T4 effect, as revealed via molecular docking simulation and ELISA. Moreover, the expression levels of key genes related to thyroid effects in zebrafish induced by TIPP and TCIPP differed from those of CDP (Fig. S9). Notably, the differences in the modes of action of OPEs in this study were consistent with previous research on nuclear/membrane THR, suggesting that the patterns of GH3 cell proliferation induced by alkyl and chlorine OPEs differed from those of aryl OPEs [62]. Based on the results of previous studies, the present results of the competitive inhibition assay demonstrated that OPEs and T4 might be competitive in binding to membrane receptor integrin $\alpha_v\beta_3$ to enter GH3 cells (Fig. 6) [49]. Therefore, TIPP and TCIPP may play a dominant role in the competition with T4 and be the main T4 inhibitors. Although CDP was an inhibitor of

cell proliferation, co-exposure with T4 can significantly promote cell proliferation at a high concentration of CDP.

## 5. Conclusions

In conclusion, the mechanism of toxicity and adverse outcome pathway of thyroid disruption of zebrafish exposed to OPEs were clarified in this study. The results of this study showed that OPEs could be typical environmental endocrine disruptors affecting TH in aquatic organisms. OPEs mainly bound to TTR (aryl OPEs: hydrogen bonding, alkyl and chlorine OPEs: non-hydrogen bonding) were transported to the target organ (the brain) via the blood–brain barrier. OPEs competed with T4 to bind to integrin $\alpha_v\beta_3$ to enter cells. Zebrafish growth was inhibited by OPEs via affecting TH endocrine function accompanied by neurodevelopment and lipid regulation, including thyroid hormone receptor binding, thyroid hormone generation, thyroid hormone transmembrane transporter activity, biosynthesis and metabolism of lipids, and neuroactive ligand–receptor interaction. However, the correlations between TH endocrine function and neurodevelopment or lipid regulation require further elucidation, and the molecular modes of action between lipid regulation and the change of body mass of zebrafish induced by OPEs also remain largely unclear. Given that the mechanism behind the toxicity of TH endocrine disruption induced by OPEs was elaborated in zebrafish, this study not only provides a basis for understanding the mechanism by which OPEs threaten aquatic organisms, but also provides a valuable theoretical basis for deriving water quality criteria and ecological risk assessment of OPEs.

## Declaration of competing interest

The authors declare that there were no known competing financial interests or personal relationships that could have appeared to influence the work reported in this paper.

## Acknowledgments

This research was financially supported by National Key Research and Development Program of China, China (2021YFC3200104), National Natural Science Foundation of China (41773085 and 41977364), and Beijing Outstanding Talent Training Program. Prof. Giesy was supported by the "High Level Foreign Experts" program (#GDT20143200016) funded by the State Administration of Foreign Experts Affairs, China, to Nanjing University, and the Einstein Professor Program of the Chinese Academy of Sciences. He was also supported by the Canada Research Chair program and a Distinguished Visiting Professorship at the Department of Environmental Sciences at Baylor University, Waco, Texas, United States.

## Appendix A. Supplementary data

Supplementary data related to this article can be found at https://doi.org/10.1016/j.ese.2022.100198.

## References

[1] S.T. Lazar, T.J. Kolibaba, J.C. Grunlan, Flame-retardant surface treatments, Nat. Rev. Mater. 5 (4) (2020) 259–275, https://doi.org/10.1038/s41578-019-0164-6.
[2] X. Li, N. Li, K. Rao, Q. Huang, M. Ma, In vitro immunotoxicity of organophosphate flame retardants in human THP-1-derived macrophages, Environ. Sci. Technol. 54 (14) (2020b) 8900–8908, https://doi.org/10.1021/acs.est.0c01152.
[3] I. van der Veen, J. de Boer, Phosphorus flame retardants: properties, production, environmental occurrence, toxicity and analysis, Chemosphere 88 (10) (2012) 1119–1153, https://doi.org/10.1016/j.chemosphere.2012.03.067.
[4] A.K. Greaves, R.J. Letcher, Comparative body compartment composition and in ovo transfer of organophosphate flame retardants in North American Great Lakes herring gulls, Environ. Sci. Technol. 48 (14) (2014) 7942–7950, https://doi.org/10.1021/es501334w.
[5] B.K. Schindler, K. Forster, J. Angerer, Determination of human urinary organophosphate flame retardant metabolites by solid-phase extraction and gas chromatography-tandem mass spectrometry, J. Chromatogr. B 877 (4) (2009) 375–381, https://doi.org/10.1016/j.jchromb.2008.12.030.
[6] G. Wei, D. Li, M. Zhuo, Y. Liao, Z. Xie, T. Guo, J. Li, S. Zhang, Z. Liang, Organophosphorus flame retardants and plasticizers: sources, occurrence, toxicity and human exposure, Environ. Pollut. 196 (2015) 29–46, https://doi.org/10.1016/j.envpol.2014.09.012.
[7] E.D. Schreder, N. Uding, M.J. La Guardia, Inhalation a significant exposure route for chlorinated organophosphate flame retardants, Chemosphere 150 (2016) 499–504, https://doi.org/10.1016/j.chemosphere.2015.11.084.
[8] A. Bacaloni, C. Cavaliere, P. Foglia, M. Nazzari, R. Samperi, A. Lagana, Liquid chromatography/tandem mass spectrometry determination of organophosphorus flame retardants and plasticizers in drinking and surface waters, Rapid Commun. Mass Spectrom. 21 (7) (2007) 1123–1130, https://doi.org/10.1002/rcm.2937.
[9] M.K. Björnsdotter, E. Romera-García, J. Borrull, J. de Boer, S. Rubio, A. Ballesteros-Gómez, Presence of diphenyl phosphate and aryl-phosphate flame retardants in indoor dust from different microenvironments in Spain and The Netherlands and estimation of human exposure, Environ. Int. 112 (2018) 59–67, https://doi.org/10.1016/j.envint.2017.11.028.
[10] L. Gao, Y. Shi, W. Li, J. Liu, Y. Cai, Occurrence and distribution of organophosphate triesters and diesters in sludge from sewage treatment plants of Beijing, China, Sci. Total Environ. 544 (2016) 143–149, https://doi.org/10.1016/j.scitotenv.2015.11.094.
[11] Y. Shi, L. Gao, W. Li, Y. Wang, J. Liu, Y. Cai, Occurrence, distribution and seasonal variation of organophosphate flame retardants and plasticizers in urban surface water in Beijing, China, Environ. Pollut. 209 (2016) 1–10, https://doi.org/10.1016/j.envpol.2015.11.008.
[12] H. Tan, D. Chen, C. Peng, X. Liu, Y. Wu, X. Li, R. Du, B. Wang, Y. Guo, E.Y. Zeng, Traditional organophosphate esters in house dust from South China: Association with hand wipes and exposure estimation, Environ. Sci. Technol. 52 (19) (2018. Novel) 11017–11026, https://doi.org/10.1021/acs.est.8b02933.
[13] F. Zhao, M. Chen, F. Gao, H. Shen, J. Hu, Organophosphorus flame retardants in pregnant women and their transfer to chorionic villi, Environ. Sci. Technol. 51 (11) (2017) 6489–6497, https://doi.org/10.1021/acs.est.7b01122.
[14] H. Zhao, F. Zhao, J. Liu, S. Zhang, D. Mu, L. An, Y. Wan, J. Hu, Trophic transfer of organophosphorus flame retardants in a lake food web, Environ. Pollut. 242 (2018) 1887–1893, https://doi.org/10.1016/j.envpol.2018.07.077.
[15] J. Fu, K. Fu, Y. Chen, X. Li, T. Ye, K. Gao, W. Pan, A. Zhang, J. Fu, Long-range transport, trophic transfer, and ecological risks of organophosphate esters in remote areas, Environ. Sci. Technol. 55 (15) (2021) 10192–10209, https://doi.org/10.1021/acs.est.0c08822.
[16] Y. Ma, Z. Xie, R. Lohmann, W. Mi, G. Gao, Organophosphate ester flame retardants and plasticizers in ocean sediments from the north Pacific to the arctic ocean, Environ. Sci. Technol. 51 (7) (2017) 3809–3815, https://doi.org/10.1021/acs.est.7b00755.
[17] A. Möller, Z. Xie, A. Caba, R. Sturm, R. Ebinghaus, Organophosphorus flame retardants and plasticizers in the atmosphere of the North Sea, Environ. Pollut. 159 (12) (2011) 3660–3665, https://doi.org/10.1016/j.envpol.2011.07.022.
[18] A. Möller, R. Sturm, Z. Xie, M. Cai, J. He, R. Ebinghaus, Organophosphorus flame retardants and plasticizers in airborne particles over the Northern Pacific and Indian Ocean toward the Polar Regions: evidence for global occurrence, Environ. Sci. Technol. 46 (6) (2012) 3127–3134, https://doi.org/10.1021/es204272v.
[19] Z. Yan, X. Jin, D. Liu, Y. Hong, W. Liao, C. Feng, Y. Bai, The potential connections of adverse outcome pathways with the hazard identifications of typical organophosphate esters based on toxicity mechanisms, Chemosphere 266 (2021b), 128989, https://doi.org/10.1016/j.chemosphere.2020.128989.
[20] J. An, J. Hu, Y. Shang, Y. Zhong, X. Zhang, Z. Yu, The cytotoxicity of organophosphate flame retardants on HepG2, A549 and Caco-2 cells, J. Environ. Sci. Health 51 (11) (2016) 980–988, https://doi.org/10.1080/10934529.2016.1191819.
[21] Z. Du, G. Wang, S. Gao, Z. Wang, Aryl organophosphate flame retardants induced cardiotoxicity during zebrafish embryogenesis: by disturbing expression of the transcriptional regulators, Aquat. Toxicol. 161 (2015) 25–32, https://doi.org/10.1016/j.aquatox.2015.01.027.
[22] K.J. Fernie, V. Palace, L.E. Peters, N. Basu, R.J. Letcher, N.K. Karouna-Renier, S.L. Schultz, R.S. Lazarus, B.A. Rattner, Investigating endocrine and physiological parameters of captive American kestrels exposed by diet to selected organophosphate flame retardants, Environ. Sci. Technol. 49 (12) (2015) 7448–7455, https://doi.org/10.1021/acs.est.5b00857.
[23] R. Li, H. Wang, C. Mi, C. Feng, L. Zhang, L. Yang, B. Zhou, The adverse effect of TCIPP and TCEP on neurodevelopment of zebrafish embryos/larvae, Chemosphere 220 (2019) 811–817, https://doi.org/10.1016/j.chemosphere.2018.12.198.
[24] S.P. McGee, E.M. Cooper, H.M. Stapleton, D.C. Volz, Early zebrafish embryogenesis is susceptible to developmental TDCPP exposure, Environ. Health Perspect. 120 (11) (2012) 1585–1591, https://doi.org/10.1289/ehp.1205316.
[25] Q. Wang, N. Lai, X. Wang, Y. Guo, P.K. Lam, J.C. Lam, B. Zhou, Bioconcentration

and transfer of the organophorous flame retardant 1,3-dichloro-2-propyl phosphate causes thyroid endocrine disruption and developmental neurotoxicity in zebrafish larvae, Environ. Sci. Technol. 49 (8) (2015) 5123–5132, https://doi.org/10.1021/acs.est.5b00558.
[26] A.C. Johnson, X. Jin, N. Nakada, J.P. Sumpter, Learning from the past and considering the future of chemicals in the environment, Science 367 (2020) 384–387, https://doi.org/10.1126/science.aay6637.
[27] X. Liu, K. Ji, K. Choi, Endocrine disruption potentials of organophosphate flame retardants and related mechanisms in H295R and MVLN cell lines and in zebrafish, Aquat. Toxicol. 114–115 (2012) 173–181, https://doi.org/10.1016/j.aquatox.2012.02.019.
[28] X. Liu, K. Ji, A. Jo, H.B. Moon, K. Choi, Effects of TDCPP or TPP on gene transcriptions and hormones of HPG axis, and their consequences on reproduction in adult zebrafish (Danio rerio), Aquat. Toxicol. 134–135 (2013) 104–111, https://doi.org/10.1016/j.aquatox.2013.03.013.
[29] Q. Wang, K. Liang, J. Liu, L. Yang, Y. Guo, C. Liu, B. Zhou, Exposure of zebrafish embryos/larvae to TDCPP alters concentrations of thyroid hormones and transcriptions of genes involved in the hypothalamic–pituitary–thyroid axis, Aquat. Toxicol. 126 (2013) 207–213, https://doi.org/10.1016/j.aquatox.2012.11.009.
[30] Q. Xu, D. Wu, Y. Dang, L. Yu, C. Liu, J. Wang, Reproduction impairment and endocrine disruption in adult zebrafish (Danio rerio) after waterborne exposure to TBOEP, Aquat. Toxicol. 182 (2017) 163–171, https://doi.org/10.1016/j.aquatox.2016.11.019.
[31] L. Yuan, J. Li, J. Zha, Z. Wang, Targeting neurotrophic factors and their receptors, but not cholinesterase or neurotransmitter, in the neurotoxicity of TDCPP in Chinese rare minnow adults (Gobiocypris rarus), Environ. Pollut. 208 (2016) 670–677, https://doi.org/10.1016/j.envpol.2015.10.045.
[32] Y. Zhu, X. Ma, G. Su, L. Yu, R.J. Letcher, J. Hou, H. Yu, J.P. Giesy, C. Liu, Environmentally relevant concentrations of the flame retardant tris(1,3-dichloro-2-propyl) phosphate inhibit growth of female zebrafish and decrease fecundity, Environ. Sci. Technol. 49 (24) (2015) 14579–14587, https://doi.org/10.1021/acs.est.5b03849.
[33] G.T. Ankley, D.C. Bencic, M.S. Breen, T.W. Collette, R.B. Conolly, N.D. Denslow, S.W. Edwards, D.R. Ekman, N. Garcia-Reyero, K.M. Jensen, J.M. Lazorchak, D. Martinovic, D.H. Miller, E.J. Perkins, E.F. Orlando, D.L. Villeneuve, R. Wang, K.H. Watanabe, Endocrine disrupting chemicals in fish: developing exposure indicators and predictive models of effects based on mechanism of action, Aquat. Toxicol. 92 (3) (2009) 168–178, https://doi.org/10.1016/j.aquatox.2009.01.013.
[34] F. Sánchez-Bayo, K.A.G. Wyckhuys, Worldwide decline of the entomofauna: a review of its drivers, Biol. Conserv. 232 (2019) 8–27, https://doi.org/10.1016/j.biocon.2019.01.020.
[35] W. Shi, X. Hu, F. Zhang, G. Hu, Y. Hao, X. Zhang, H. Liu, S. Wei, X. Wang, J.P. Giesy, H. Yu, Occurrence of thyroid hormone activities in drinking water from eastern China: contributions of phthalate esters, Environ. Sci. Technol. 46 (3) (2012a) 1811–1818, https://doi.org/10.1021/es202625r.
[36] P.J. Van den Brink, A.C. Alexander, M. Desrosiers, W. Goedkoop, P.L. Goethals, M. Liess, S.D. Dyer, Traits-based approaches in bioassessment and ecological risk assessment: strengths, weaknesses, opportunities and threats, Integrated Environ. Assess. Manag. 7 (2) (2011) 198–208, https://doi.org/10.1002/ieam.109.
[37] S. Kim, J. Jung, I. Lee, D. Jung, H. Youn, k Choi, Thyroid disruption by triphenyl phosphate an organophosphate flame retardant in zebrafish (Danio rerio) embryos larvae and in GH3 and FRTL-5 cell lines, Aquat. Toxicol. 160 (2015) 188–196, https://doi.org/10.1016/j.aquatox.2015.01.016.
[38] Z. Dang, M. Arena, A. Kienzler, Fish toxicity testing for identification of thyroid disrupting chemicals, Environ. Pollut. 284 (2021), https://doi.org/10.1016/j.envpol.2021.117374.
[39] Z. Han, Y. Li, S. Zhang, N. Song, H. Xu, Y. Dang, C. Liu, J.P. Giesy, H. Yu, Prenatal transfer of decabromodiphenyl ether (BDE-209) results in disruption of the thyroid system and developmental toxicity in zebrafish offspring, Aquat. Toxicol. 190 (2017) 46–52, https://doi.org/10.1016/j.aquatox.2017.06.020.
[40] D. Knapen, E. Stinckens, J.E. Cavallin, G.T. Ankley, H. Holbech, D.L. Villeneuve, L. Vergauwen, Toward an AOP network-based tiered testing strategy for the assessment of thyroid hormone disruption, Environ. Sci. Technol. 54 (14) (2020) 8491–8499, https://doi.org/10.1021/acs.est.9b07205.
[41] W. Shi, F. Zhang, G. Hu, Y. Hao, X. Zhang, H. Liu, S. Wei, X. Wang, J.P. Giesy, H. Yu, Thyroid hormone disrupting activities associated with phthalate esters in water sources from Yangtze River Delta, Environ. Int. 42 (2012b) 117–123, https://doi.org/10.1016/j.envint.2011.05.013.
[42] X. Zheng, Y. Zhu, C. Liu, H. Liu, J.P. Giesy, M. Hecker, M.H. Lam, H. Yu, Accumulation and biotransformation of BDE-47 by zebrafish larvae and teratogenicity and expression of genes along the hypothalamus-pituitary-thyroid axis, Environ. Sci. Technol. 46 (23) (2012) 12943–12951, https://doi.org/10.1021/es303289n.
[43] Q. Zhang, C. Ji, X. Yin, L. Yan, M. Lu, M. Zhao, Thyroid hormone-disrupting activity and ecological risk assessment of phosphorus-containing flame retardants by in vitro, in vivo and in silico approaches, Environ. Pollut. 210 (2016) 27–33, https://doi.org/10.1016/j.envpol.2015.11.051.
[44] Q. Shi, M. Wang, F. Shi, L. Yang, Y. Guo, C. Feng, J. Liu, B. Zhou, Developmental neurotoxicity of triphenyl phosphate in zebrafish larvae, Aquat. Toxicol. 203 (2018) 80–87, https://doi.org/10.1016/j.aquatox.2018.08.001.
[45] L. Sun, H. Tan, T. Peng, S. Wang, W. Xu, H. Qian, Y. Jin, Z. Fu, Developmental neurotoxicity of organophosphate flame retardants in early life stages of Japanese medaka (Oryzias latipes), Environ. Toxicol. Chem. 35 (12) (2016) 2931–2940, https://doi.org/10.1002/etc.3477.
[46] Q. Chen, X. Wang, W. Shi, H. Yu, X. Zhang, J.P. Giesy, Identification of thyroid hormone disruptors among HO-PBDEs: in vitro investigations and coregulator involved simulations, Environ. Sci. Technol. 50 (22) (2016) 12429–12438, https://doi.org/10.1021/acs.est.6b02029.
[47] A.C. Gutleb, I.A. Meerts, J.H. Bergsma, M. Schriks, A.J. Murk, T-Screen as a tool to identify thyroid hormone receptor active compounds, Environ. Toxicol. Pharmacol. 19 (2) (2005) 231–238, https://doi.org/10.1016/j.etap.2004.06.003.
[48] N. Li, W. Jiang, M. Ma, D. Wang, Z. Wang, Chlorination by-products of bisphenol A enhanced retinoid X receptor disrupting effects, J. Hazard Mater. 320 (2016) 289–295, https://doi.org/10.1016/j.jhazmat.2016.08.033.
[49] J. Li, H. Liu, R. Zuo, J. Yang, N. Li, Competitive binding assays for measuring the binding affinity of thyroid-disrupting chemicals for integrin alphavbeta3, Chemosphere 249 (2020a), 126034, https://doi.org/10.1016/j.chemosphere.2020.126034.
[50] K.M. Crofton, Thyroid disrupting chemicals: mechanisms and mixtures, Int. J. Androl. 31 (2) (2008) 209–223, https://doi.org/10.1111/j.1365-2605.2007.00857.x.
[51] A.J. Murk, E. Rijntjes, B.J. Blaauboer, R. Clewell, K.M. Crofton, M.M.L. Dingemans, J. David Furlow, R. Kavlock, J. Köhrle, R. Opitz, T. Traas, T.J. Visser, M. Xia, A.C. Gutleb, Mechanism-based testing strategy using in vitro approaches for identification of thyroid hormone disrupting chemicals, Toxicol. Vitro 27 (4) (2013) 1320–1346, https://doi.org/10.1016/j.tiv.2013.02.012.
[52] R. Chen, R. Hou, X. Hong, S. Yan, J. Zha, Organophosphate flame retardants (OPFRs) induce genotoxicity in vivo: a survey on apoptosis, DNA methylation, DNA oxidative damage, liver metabolites, and transcriptomics, Environ. Int. 130 (2019), 104914, https://doi.org/10.1016/j.envint.2019.104914.
[53] Z. Yan, C. Feng, X. Jin, D. Liu, Y. Hong, Y. Qiao, Y. Bai, H.B. Moon, A. Qadeer, F. Wu, In vitro metabolic kinetics of cresyl diphenyl phosphate (CDP) in liver microsomes of crucian carp (Carassius carassius), Environ. Pollut. 274 (2021a), 116586, https://doi.org/10.1016/j.envpol.2021.116586.
[54] B. Czarnocka, Thyroperoxidase, thyroglobulin, Na+/I- symporter, pendrin in thyroid autoimmunity, Front. Biosci. 16 (1) (2011) 783–802, https://doi.org/10.2741/3720.
[55] L. Fayadat, P. Niccoli-Sire, J. Lanet, J.L. Franc, Human thyroperoxidase is largely retained and rapidly degraded in the endoplasmic reticulum. Its N-glycans are required for folding and intracellular trafficking, Endocrinology 139 (10) (1998) 4277–4285, https://doi.org/10.1210/en.139.10.4277.
[56] K. Suzuki, S. Lavaroni, A. Mori, M. Ohta, J. Saito, M. Pietrarelli, D.S. Singer, S. Kimura, R. Katoh, A. Kawaoi, L.D. Kohn, Autoregulation of thyroid-specific gene transcription by thyroglobulin, Proc. Natl. Acad. Sci. U.S.A. 95 (14) (1998) 8251–8256, https://doi.org/10.1073/pnas.95.14.8251.
[57] A. Taurog, M.L. Dorris, L. Lamas, Comparison of lactoperoxidase- and thyroid peroxidase-catalyzed iodination and coupling, Endocrinology 94 (1974) 1286–1294, https://doi.org/10.1210/endo-94-5-1286.
[58] M. Ehlers, A. Thiel, C. Bernecker, D. Porwol, C. Papewalis, H.S. Willenberg, S. Schinner, H. Hautzel, W.A. Scherbaum, M. Schott, Evidence of a combined cytotoxic thyroglobulin and thyroperoxidase epitope-specific cellular immunity in Hashimoto's thyroiditis, J. Clin. Endocrinol. Metab. 97 (4) (2012) 1347–1354, https://doi.org/10.1210/jc.2011-2178.
[59] A. Sánchez, R. Cardona, M. Munera, J. Sánchez, Identification of antigenic epitopes of thyroperoxidase, thyroglobulin and interleukin-24. Exploration of cross-reactivity with environmental allergens and possible role in urticaria and hypothyroidism, Immunol. Lett. 220 (2020) 71–78, https://doi.org/10.1016/j.imlet.2020.02.003.
[60] K.L. Howdeshell, A model of the development of the brain as a construct of the thyroid system, Environ. Health Perspect. 110 (2002) 337–348, https://doi.org/10.1289/ehp.02110s3337.
[61] S.P. Porterfield, Thyroidal dysfunction and environmental chemicals–potential impact on brain development, Environ. Health Perspect. 108 (3) (2000) 433–438, https://doi.org/10.1289/ehp.00108s3433.
[62] J. Li, Y. Xu, N. Li, R. Zuo, Y. Zhai, H. Chen, Thyroid hormone disruption by organophosphate esters is mediated by nuclear/membrane thyroid hormone receptors: in vitro, in vivo, and in silico studies, Environ. Sci. Technol. 56 (7) (2022) 4241–4250, https://doi.org/10.1021/acs.est.1c05956.
[63] S. Fakas, Lipid biosynthesis in yeasts: a comparison of the lipid biosynthetic pathway between the model nonoleaginous yeast Saccharomyces cerevisiae and the model oleaginous yeast Yarrowia lipolytica, Eng. Life Sci. 17 (3) (2017) 292–302, https://doi.org/10.1002/elsc.201600040.
[64] X. Miao, Q. Luo, X. Qin, Y. Guo, H. Zhao, Genome-wide mRNA-seq profiling reveals predominant down-regulation of lipid metabolic processes in adipose tissues of Small Tail Han than Dorset sheep, Biochem. Biophys. Res. Commun. 467 (2) (2015) 413–420, https://doi.org/10.1016/j.bbrc.2015.09.129.
[65] X. Wang, Y. Ma, J. Liu, X. Yin, Z. Zhang, C. Wang, Y. Li, H. Wang, Reproductive toxicity of beta-diketone antibiotic mixtures to zebrafish (Danio rerio), Ecotoxicol. Environ. Saf. 141 (2017) 160–170, https://doi.org/10.1016/j.ecoenv.2017.02.042.
[66] I. Fuertes, R. Jordao, B. Pina, C. Barata, Time-dependent transcriptomic responses of Daphnia magna exposed to metabolic disruptors that enhanced storage lipid accumulation, Environ. Pollut. 249 (2019) 99–108, https://doi.org/10.1016/j.envpol.2019.02.102.
[67] N. Caporale, M. Leemans, L. Birgersson, P.L. Germain, C. Cheroni, G. Borbély, E. Engdahl, C. Lindh, R.B. Bressan, F. Cavallo, N.E. Chorev, G.A. D'Agostino,

S.M. Pollard, M.T. Rigoli, E. Tenderini, A.L. Tobon, S. Trattaro, F. Troglio, M. Zanella, Å. Bergman, P. Damdimopoulou, M. Jönsson, W. Kiess, E. Kitraki, H. Kiviranta, E. Nånberg, M. Öberg, P. Rantakokko, C. Rudén, O. Söder, C.-G. Bornehag, B. Demeneix, J.-B. Fini, C. Gennings, J. Rüegg, J. Sturve, G. Testa, From cohorts to molecules: adverse impacts of endocrine disrupting mixtures, Science 375 (6582) (2022), https://doi.org/10.1126/science.abe8244.

[68] O. Dohan, Z. Baloch, Z. Banrevi, V. Livolsi, N. Carrasco, Predominant intracellular overexpression of the Na (+)/I (-) symporter (NIS) in a large sampling of thyroid cancer cases, J. Clin. Endocrinol. Metab. 86 (6) (2001) 2697–2700, https://doi.org/10.1210/jc.86.6.2697.

[69] M.A. Beg, I.A. Sheikh, Endocrine disruption: molecular interactions of environmental bisphenol contaminants with thyroid hormone receptor and thyroxine-binding globulin, Toxicol. Ind. Health 36 (5) (2020) 322–335, https://doi.org/10.1177/0748233720928165.

[70] J.H. Oppenheimer, Role of plasma proteins in the binding, distribution and metabolism of the thyroid hormones, N. Engl. J. Med. 278 (21) (1968) 1153–1162, https://doi.org/10.1056/NEJM196805232782107.

[71] J.P. Chanoine, S. Alex, S.L. Fang, S. Stone, J.L. Leonard, J. Körhle, L.E. Braverman, Role of transthyretin in the transport of thyroxine from the blood to the choroid plexus, the cerebrospinal fluid, and the brain, Endocrinology 130 (2) (1992) 933–938, https://doi.org/10.1210/en.130.2.933.

[72] Q. Chi, W. Zhang, L. Wang, J. Huang, M. Yuan, H. Xiao, X. Wang, Evaluation of structurally different brominated flame retardants interacting with the transthyretin and their toxicity on HepG2 cells, Chemosphere 246 (2020), https://doi.org/10.1016/j.chemosphere.2019.125749.

[73] G. Schreiber, A.R. Aldred, A. Jaworowski, C. Nilsson, M.G. Achen, M.B. Segal, Thyroxine transport from blood to brain via transthyretin synthesis in choroid plexus, Am. J. Physiol. 258 (Pt 2) (1990) R338–R345, https://doi.org/10.1152/ajpregu.1990.258.2.R338.

[74] T. Pappa, A.M. Ferrara, S. Refetoff, Inherited defects of thyroxine-binding proteins, Best Pract. Res. Clin. Endocrinol. Metabol. 29 (5) (2015) 735–747, https://doi.org/10.1016/j.beem.2015.09.002.

[75] W.P. Qin, C.H. Li, L.H. Guo, X.M. Ren, J.Q. Zhang, Binding and activity of polybrominated diphenyl ether sulfates to thyroid hormone transport proteins and nuclear receptors, Environ. Sci. Process. Impacts. 21 (6) (2019) 950–956, https://doi.org/10.1039/c9em00095j.

[76] M. Besson, W.E. Feeney, I. Moniz, L. Francois, R.M. Brooker, G. Holzer, M. Metian, N. Roux, V. Laudet, D. Lecchini, Anthropogenic stressors impact fish sensory development and survival via thyroid disruption, Nat. Commun. (2020), https://doi.org/10.1038/s41467-020-17450-8.

[77] K.M. Gabrielsen, J.S. Krokstad, G.D. Villanger, D.A. Blair, M.J. Obregon, C. Sonne, R. Dietz, R.J. Letcher, B.M. Jenssen, Thyroid hormones and deiodinase activity in plasma and tissues in relation to high levels of organohalogen contaminants in East Greenland polar bears (Ursus maritimus), Environ. Res. 136 (2015) 413–423, https://doi.org/10.1016/j.envres.2014.09.019.

[78] R. Guyot, F. Chatonnet, B. Gillet, S. Hughes, F. Flamant, Toxicogenomic analysis of the ability of brominated flame retardants TBBPA and BDE-209 to disrupt thyroid hormone signaling in neural cells, Toxicology 325 (2014) 125–132, https://doi.org/10.1016/j.tox.2014.08.007.

[79] H. Kojima, S. Takeuchi, N. Uramaru, K. Sugihara, T. Yoshida, S. Kitamura, Nuclear hormone receptor activity of polybrominated diphenyl ethers and their hydroxylated and methoxylated metabolites in transactivation assays using Chinese hamster ovary cells, Environ. Health Perspect. 117 (8) (2009) 1210–1218, https://doi.org/10.1289/ehp.0900753.

[80] L. Yu, Z. Han, C. Liu, A review on the effects of PBDEs on thyroid and reproduction systems in fish, Gen. Comp. Endocrinol. 219 (2015) 64–73, https://doi.org/10.1016/j.ygcen.2014.12.010.

# Organophosphate esters cause thyroid dysfunction via multiple signaling pathways in zebrafish brain

Zhenfei Yan[a,b], Chenglian feng[a, *], Xiaowei Jin[c, *], Fangkun Wang[d], Cong Liu[d], Na Li[e], Yu Qiao[a], Yingchen Bai[a], Fengchang Wu[a,b], John P. Giesy[f,g,h]

[a] State Key Laboratory of Environmental Criteria and Risk Assessment, Chinese Research Academy of Environmental Sciences, Beijing, 100012, China

[b] College of Environment, Hohai University, Nanjing, 210098, China

[c] China National Environmental Monitoring Centre, Beijing, 100012, China

[d] Department of Preventive Veterinary Medicine, College of Veterinary Medicine, Shandong Agricultural University, Taian, 271018, China

[e] Key Laboratory of Drinking Water Science and Technology, Research Center for Eco-Environmental Sciences, Chinese Academy of Sciences, Beijing 100085, China

[f] Department of Veterinary Biomedical Sciences, University of Saskatchewan, Saskatoon, SK, Canada

[g] Toxicology Centre, University of Saskatchewan, Saskatoon, Saskatchewan, Canada

[h] Department of Environmental Sciences, Baylor University, Waco, Texas, USA

**Supporting Information**

## SI Pretreatment and Quantification of TIPP, CDP, and TCIPP in Exposure Solutions and in Tissues Using HPLC-MS/MS

Exposure solutions were monitored to assure accuracy of doing. Samples collected during this study were pre-concentrated according to previously published research with minor modifications (Wang et al., 2011). All samples of exposure solution were filtered through 0.45 μm filter then extracted by Oasis HLB column (Waters Corporation, Milford, MA, USA). HLB cartridges were sequentially activated with 5 mL acetonitrile and 5 mL ultrapure water, following loading with a flow rate of 1 mL·min-1. Columns were then rinsed with 10 mL ultrapure water, dried for 20 min, and finally eluted with 10 mL acetonitrile. Eluents were evaporated to nearly 100 μL under gentle nitrogen (at 37 ℃) and diluted to 1 mL with acetonitrile. The final diluents were filtered through a 0.22 μm, minisart syringe filter (Sartorius, Göttingen, Germany) and stored at -20 ℃ until analyzed by use of high-performance liquid chromatograph mass spectrometer.

Tissue of zebrafish exposed to OPEs were also quantified in this study, and pretreated based on these previous researches with minor modifications (Hou et al., 2019; Zhu et al., 2015). Zebrafish muscle tissue were weighed and homogenized, in which 10 ng of TCEP-d12 as internal standard for OPEs and 3 g of anhydrous sodium sulfate ($Na_2SO_4$) were spiked. The homogenates with 3 mL of dichloromethane/n-hexane (DCM/HEX) mixture (1:1, v/v) after vortex mixed for 1 min the ultrasonicated for 30 min at room temperature, centrifuged at 5 000 × g for 10 min, and supernatant transferred into a new centrifuge tube. The above process was conducted a mixture of DCM/HEX (1:1, v/v) two times and supernatants combined. Extracts were concentrated to dryness under a gentle stream of nitrogen gas, and the residue was re-dissolved in 2 mL of HEX after centrifuge tubes were re-weighed to determine lipid weight of the fish tissues. The re-dissolved samples were loaded onto a SPE-$NH_2$ cartridge (Sep-Pak, 500mg, 3 mL, Waters) pre-activated with 3 mL DCM/HEX (1:1, v/v), 6 mL DCM, and 6 mL HEX. After rinsing cartridge with 5 mL DCM/HEX (1:4, v/v), the following targets OPEs TIPP, CDP, TCIPP, and TCEP-d12 were eluted with 3 mL DCM/HEX (1:4,

v/v), 8 mL DCM, and 4 mL DCM/methanol (9:1, v/v) at a flow rate of 0.5 $mL \cdot min^{-1}$. The eluent was concentrated nearly to dryness and diluted in 200 μL acetonitrile. The diluent was filtered through a 0.22 μm filter and stored at -20℃ until analysis.

Quantification of OPEs after pretreatment was performed by use of high-performance liquid chromatograph mass spectrometer (HPLC-MS/MS, Nexera-X2/8040) Shimadzu Co. Ltd. with a Waters C18 column (50 mm × 2.1 mm, 3.5 mm), using a multiple reaction monitoring (MRM) model in positive ionization electrospray mode (ESI+). Injection volumes were 5 μL, and the column temperature was set at 40 ℃. The binary mobile phase consisted of 0.1% formic acid in water (A) and acetonitrile (B) at a flow rate of 0.2 $mL \cdot min^{-1}$. The gradient elution was set as follows: 0 min 40% B, 4 min 80% B, 5 min 80% B, 5.5 min 100% B, 6 min 100% B, 6.5 min 40% B, 7 min 40% B. The detailed information regarding MRM transitions and MS conditions was provided in Table S1 and Figure S1.

The QA/QC procedure undertaken in this study included background contamination and recoveries of OPEs. During quantification of TIPP, TCIPP, and CDP in exposure solution, no background contamination was detected. However, background contamination of CDP in tissues was detected and less than its limit of detection (LOD), but not for TIPP and TCIPP. The LODs of TIPP, TCIPP, and CDP used in exposure solution and tissues were 3-fold greater than the signal-to-noise ratio (Table S1). In this study, recoveries of TIPP, TCIPP, and CDP in exposure solution and biota samples were 58.2% – 108.4%, 85.1% – 120.9%, and 74.0% – 111.3%, respectively. In addition, the standard curves $R^2$ of TIPP, TCIPP, and CDP were all greater than 0.99. The limits of quantification (LOQs) of TIPP, TCIPP, and CDP in exposure solution and biota samples can generate instrumental response that set as 10 times the signal-to-noise ratio (Table S1).

No OPEs were detected in control solutions, and there was no significant difference between the administered concentrations and the measured concentrations of OPEs before and after renewing exposure solutions (Table S2). Thus, it was suggested that the accuracy of the chronic study and the credibility of these research results were guaranteed. Concentrations of TIPP, CDP and TCIPP in fish tissues were quantified and

concentrations of TIPP and TCIPP determined in tissue homogenates of zebrafish collected from these groups exposed to 10 μg·L$^{-1}$, 50 μg·L$^{-1}$, and 100 μg·L$^{-1}$ were not detected, and the parts were less than their LOQ. While the levels of TCIPP exposed to 100 μg·L$^{-1}$ was 20.99 ± 7.31 μg·kg$^{-1}$ wet mass (ww) in tissue. However, concentrations of CDP in tissues exposed to 10 μg·L$^{-1}$, 50 μg·L$^{-1}$ and 100 μg·L$^{-1}$ were 5.26 ± 1.90, 21.63 ± 6.42, and 27.43 ± 2.01 μg·kg$^{-1}$ wet mass (ww), respectively.

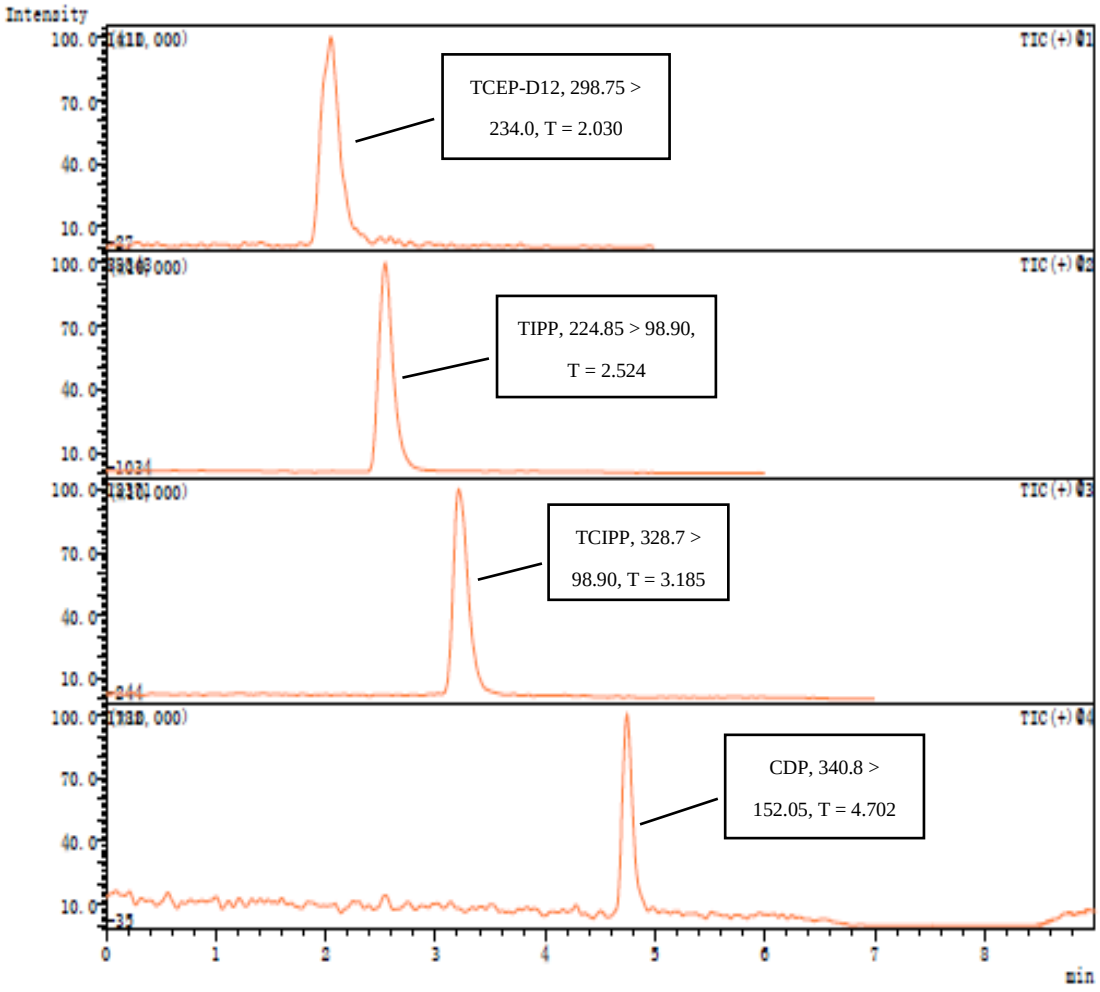


**Figure S1.** Chromatogram with some information of these OPEs using a HPLC-MS/MS.

**Table S1.** Detailed information for quantification TIPP, CDP and TCIPP using the HPLC-MS/MS with MRM transitions and ESI+ mode

| Compounds | Retention time (min) | MRM transitions | Collision energy (eV) | LOD | | LOQ | | $R^2$ of the standard curve |
|---|---|---|---|---|---|---|---|---|
| | | | | Water (μg·L$^{-1}$) | Biota (μg·kg$^{-1}$) | Water (μg·L$^{-1}$) | Biota (μg·kg$^{-1}$) | |
| TCEP-D12 | 1.47[a] | 298.75 > 234.00[c] | 15.0 | 1.26 | 1.69 | 3.81 | 5.13 | – |
| | 2.03[b] | 298.75 > 110.90 | 23.0 | | | | | |
| TIPP | 1.83[a] | 224.85 > 98.90[c] | 18.0 | 0.15 | 0.11 | 0.47 | 0.33 | 0.998 |
| | 2.52[b] | 224.85 > 125.10 | 11.0 | | | | | |
| TCIPP | 2.23[a] | 328.70 > 98.90[c] | 23.0 | 0.22 | 0.31 | 0.66 | 0.94 | 0.991 |
| | 3.18[b] | 328.60 > 124.80 | 17.0 | | | | | |
| CDP | 3.43[a] | 340.80 > 152.05[c] | 39.0 | 3.90 | 0.59 | 11.81 | 1.78 | 0.991 |
| | 4.70[b] | 340.80 > 77.10 | 47.0 | | | | | |

Note: a: Quantification of exposure solution; b: Quantification of tissues; c: Quantification transition.

**Table S2.** Concentration of TIPP, CDP, and TCIPP before and after renewing of exposure solutions and tissues after 28 d exposure.

| OPEs | Exposure solutions (μg·L$^{-1}$) | | | | | | Tissues (μg·kg$^{-1}$) | | |
|---|---|---|---|---|---|---|---|---|---|
| | Before (10) | After (10) | Before (50) | After (50) | Before (100) | After (100) | 10 μg·L$^{-1}$ | 50 μg·L$^{-1}$ | 100 μg·L$^{-1}$ |
| TIPP | 9.47 ± 0.91 | 7.68 ± 0.45 | 41.61 ± 7.09 | 42.97 ± 4.60 | 81.07 ± 6.79 | 75.94 ± 11.45 | | ND | |
| CDP | 7.83 ± 0.84 | 8.68 ± 0.42 | 45.17 ± 6.53 | 45.14 ± 4.23 | 91.83 ± 6.25 | 87.23 ± 6.72 | 5.26 ± 1.90 | 21.63 ± 6.42 | 27.43 ± 2.01 |
| TCIPP | 8.47 ± 0.01 | 11.83 ± 0.42 | 44.85 ± 4.31 | 46.03 ± 2.56 | 94.76 ± 2.49 | 90.15 ± 7.30 | ND | < LOD | 20.99 ± 7.31 |

Note: ND: not detected.

**SII Cell proliferation for 96 h based on GH3 cell lines**

GH3 cells were cultured in complete medium for 3 days after passage in order to obtain 1 ~ 5 × $10^6$ cell·mL$^{-1}$. The T-screen assay procedure exposed to OPEs and T4 for 96 h was carried out by the previous researches with minor modifications (Gutleb et al., 2005; Zhang et al., 2016). In brief, after 3 days, the complete medium was discarded, and the culture plate was rinsed one time with phosphate buffers saline before trypsinization for 1 min. The complete medium was placed into the culture plate and rocked a circle to stop the cell dissociation. Subsequently, the cells were collected from the culture plate at 1000 rpm for 5 min. The phenol red-free RPMI-1640 culture medium with 5% charcoal-dextran-treated fetal bovine serum (CD-FBS) and 1% penicillin-streptomycin was used to cultivate the cells (3500 cells/well) for 48 h in order to avoid interference by endogenous of T4. Then the cells collected from the culture flask were planted in a transparent 96-well culture plate at a density of 3500 cells per well. After that, the acute toxicity test of GH3 cells included the blank (0.1% v:v DMSO), the positive (T4), and the experimental group (OPEs) cultured in test culture medium with phenol red-free RPMI-1640, 5% CD-FBS and 1% penicillin-streptomycin. Original solutions of T4, CDP, TIPP, and TCIPP ($1.3\times10^4$ μM, $3.5\times10^6$ μM, $4.3\times10^6$ μM, and $3.88\times10^6$ μM) were diluted 10 times with DMSO, and then were diluted at 1:1000 with phenol red-free RPMI-1640 and 5% CD-FBS culture medium. After that, the preprocessed original solutions were diluted 10 times step by step to obtain the final administered concentrations of OPEs and T4 (0.1% v:v DMSO) that there were six groups, respectively. Each concentration was repeated three times, and exposed in a

transparent 96-well culture plate. During 96 h exposure, the exposure medium of these samples was refreshed every 24 h. After 96 h, the cell proliferation was measured via a microplate reader at 490 nm, which was treated with the MTS kit (Bestbio, Shanghai, China) according to the technical manual. $RIC_{20}$ and $RIC_{50}$ (the concentration of OPEs and T4 required to inhibit 20% or 50% cell proliferation comparing to the blank) were calculated by these ODs value. These values were all conducted using IBM SPSS statistics 22.0 (IBM Corporation, Armonk, NY, USA) with one-way analysis of variance and Origin 2018 (OriginLab Corporation, Northampton, MA, USA) with linear fitting analysis.

Based on acute toxicity to GH3 cells, $RIC_{20}$ of T4, CDP, TIPP, and TCIPP were $2.5\times10^{-4}$ μM, $2.4\times10^{-3}$ μM, 1.4 μM, and 1.4 μM, while $RIC_{50}$ of T4, CDP, TIPP, and TCIPP were $5.7\times10^{-2}$ μM, 0.38 μM, $1.8\times10^{3}$ μM, and 90.3 μM.

**Table S3.** The $RIC_{20}$ and $RIC_{50}$ values of T4, CDP, TIPP, and TCIPP exposure for 96 h.

| Pollutant | $RIC_{20}$ (μM) | $RIC_{50}$ (μM) |
|---|---|---|
| T4 (promote) | $2.5\times10^{-4}$ | $5.7\times10^{-2}$ |
| CDP (inhibit) | $2.4\times10^{-3}$ | 0.38 |
| TIPP (inhibit) | 1.4 | $1.8\times10^{3}$ |
| TCIPP (inhibit) | 1.4 | 90.3 |

**SIII Protein extraction and western blot analysis on GH3 cells**

Protein from GH3 cells were obtained by SDS lysis buffer (50 mM Tris-HCl (PH=6.8), 2% SDS (w/v), 0.1% bromophenol blue (w/v), 10% glycerol (v/v), 200 mM dithiothreitol), following by heated at 100 ℃ for 10 minutes and loading onto sodium dodecyl sulfate-polyacrylamide gel electrophoresis (SDS-PAGE). Proteins on SDS-PAGE gels were transferred into polyvinylidene difluoride membranes (PVDF, Millipore. R1JB31478). The membranes were blocked with phosphate buffer solution with 0.1% (v/v) Tween-20 (PBST) containing 5% skim milk for 2h at room temperature, and then incubated with the primary antibody overnight at 4 ℃ followed by the horseradish peroxidase (HRP)-conjugated goat anti-rabbit/mouse IgG secondary antibody for 1h at room temperature. Immunoreactions were detected by NcmECL Ultra (NCM Biotech. P10200). Glyceraldehyde-3-phosphate dehydrogenase (GADPH) was used as a loading control. All primary and secondary antibodies were diluted by PBST containing 2.5 % skim milk. The primary antibody including rabbit-anti rat NIS (1:1000 dilution, proteintech 24324-1-AP), rabbit-anti rat TBG (1:1000 dilution,

Cloud-Clone Crop. PAA305Ra01), rabbit-anti rat TTR (1:1000 dilution, Cloud-Clone Crop. PAA726Ra01) and mouse anti-GAPDH monoclonal antibody (1:10000 dilution, Biodragon. B1030) (Faria et al., 2020; Huang et al., 2014). Secondary antibody including HRP-conjugated goat anti-mouse IgG (1:20000 dilution, Proteintech. SA00001-1) and HRP-conjugated goat anti-rabbit IgG (1:20000 dilution, Proteintech. SA00001-2).

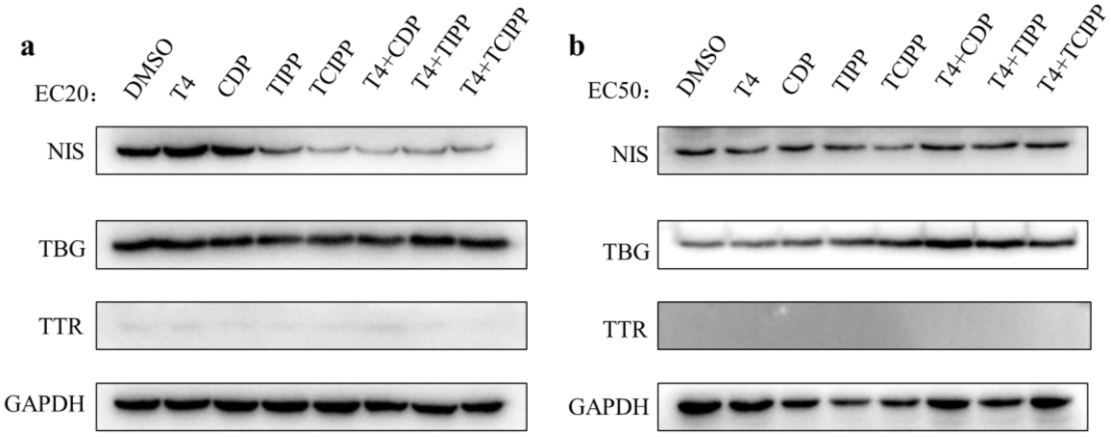


**Figure S2.** Western blot analysis of TTR, TBG, and NIS in GH3 cells after exposure to T4, CDP, TIPP, and TCIPP of EC20 (a) and EC50 (b). Glyceraldehyde 3-phosphate dehydrogenase (GAPDH) expression was used as internal reference.

**SIV Quantification of hormone concentrations**

Concentrations of T4 in blood, TTR, TBG, and NIS in brain, TPO and TG in brain and soma samples of zebrafish were quantified following previous methods through enzyme-linked immunosorbent assays (ELISA) obtained from GeneCopoeia Inc. with minor modification (Ji et al., 2013; Kim et al., 2015). Briefly, blood from each treatment was centrifuged at 3,000 × g for 30 min, and the collected supernatant was stored at -80 ℃ until measured by ELISA kit following the manufacturer′s instructions. In addition, brain and soma samples per each group with 90% (1 g tissue:9 mL buffer) PBS buffer (0.01 M, pH = 7.2 – 7.4) were homogenized by homogenizer (DWK Life Sciences, Millville, NJ, USA) in an ice bath. The homogenates were centrifuged at 5,000 × g for 15 min, thereby collecting the supernatants stored at -80 ℃ until also measured by ELISA kit following the manufacturer′s instructions.

**SV The Detailed Procedures on Transcriptome Sequencing (RNA-seq) of Brain in Zebrafish Exposed to TIPP, TCIPP, and CDP.**

Total RNA was extracted from the tissue using TRIzol® Reagent (Plant RNA Purification Reagent for plant tissue) according the manufacturer's instructions (Invitrogen) and genomic DNA was removed by DNase I (TaKara). Then RNA quality was determined by 2100 Bioanalyser (Agilent) and quantified using the ND-2000 (NanoDrop Technologies). Sequencing library was constructed by high-quality RNA sample (OD260/280 = 1.8~2.2, OD260/230 ≥ 2.0, RIN ≥ 6.5, 28S:18S ≥ 1.0, > 1 μg).

RNA-seq transcriptome library was prepared following TruSeq$^{TM}$ RNA sample preparation Kit from Illumina (San Diego, CA) using 1μg of total RNA. Shortly, messenger RNA was isolated according to polyA selection method by oligo(dT) beads and then fragmented by fragmentation buffer firstly. Secondly double-stranded cDNA was synthesized using a SuperScript double-stranded cDNA synthesis kit (Invitrogen, CA) with random hexamer primers (Illumina). Synthesized cDNA was subjected to end-repair, phosphorylation and 'A' base addition according to Illumina's library construction protocol. Libraries were size selected for cDNA target fragments of 300 bp on 2% Low Range Ultra Agarose followed by PCR amplified using Phusion DNA polymerase (NEB) for 15 PCR cycles. After quantified by TBS380, paired-end RNA-seq sequencing library was sequenced with the Illumina HiSeq xten/NovaSeq 6000 sequencer (2 × 150 bp read length).

Raw paired end reads were trimmed and quality controlled by SeqPrep (https://github.com/jstjohn/SeqPrep) and Sickle (https://github.com/najoshi/sickle) with default parameters. Then clean reads were separately aligned to reference genome with orientation mode using HISAT2 (http://ccb.jhu.edu/software/hisat2/index.shtml) software. Mapped reads of each sample were assembled by StringTie (https://ccb.jhu.edu/software/stringtie/index.shtml?t=example) in a reference-based approach.

To identify differentially expression genes (DEGs) between samples, the expression of each transcript was calculated according to the transcripts per million reads (TPM) method. RSEM (http://deweylab.biostat.wisc.edu/rsem/) was used to quantify gene abundances. Essentially, differential expression analysis was performed using the DESeq2/DEGseq/EdgeR with Q value ≤ 0.05, DEGs with |log2FC| > 1 and Q value ≤ 0.05 (DESeq2 or EdgeR)/Q value ≤ 0.001 (DEGseq) were considered to be significantly DEGs. In addition, functional-enrichment analysis including GO and KEGG were performed to identify which DEGs were significantly enriched in GO terms and metabolic pathways at Bonferroni-corrected P-value ≤ 0.05 compared with

the whole-transcriptome background. GO functional enrichment and KEGG pathway analysis were carried out by Goatools (https://github.com/tanghaibao/Goatools) and KOBAS (http://kobas.cbi.pku.edu.cn/home.do).

The results on RNA-seq in brain have shown that a total of 47,736 genes, were investigated, of which 9,793 genes were DEGs (Table S7-S16). Patterns of expression of genes in zebrafish exposed to each OPEs were all significantly different from those of controls. Results of correlation analyses among all samples were ≥ 0.8, suggesting that the research design was effective and results were reliable (Figure S5 and S6). Compared with controls, number of down-regulated genes in samples exposed to 10 μg CDP·$L^{-1}$ or 100 μg TCIPP·$L^{-1}$ were greater than up-regulation genes (Figure S7). However, exposure of zebrafish to 10 μg TIPP·$L^{-1}$ or 10 μg TCIPP·$L^{-1}$ caused more up-regulated genes than down-regulated genes. The number of down-regulated or up-regulated genes in zebrafish exposed to other groups were similar. When 91 thyroid-related genes that were selected from 47,736 genes in all samples were used for hierarchical cluster analysis (Figure S9 and Table S18), the normalized expression value of thyroid stimulating hormone beta subunit a (tshβa) was not detected in all samples. Also, 35 co-expressed genes related to thyroid function were selected from 13,975 genes that were common in each sample, and were used for hierarchical cluster (Figure S10 and Table S19).

**SVI The Detailed Procedures on Validation of Transcriptome Analysis using Quantitative Real Time PCR (qRT-PCR) of Brain in Zebrafish.**

To validated accuracy and rationality of RNA-seq analysis, qRT-PCR reactions were performed as previously described with minor modification (Kwon et al., 2016; Qiu et al., 2020; Zhu et al., 2017). In brief, total RNA was extracted and isolated according to the supporting information SV. Several specific primers for the selected target DEGs in this study were synthesized by Sangon Biotech Co., Ltd. (Shanghai, China), including the housekeeping gene ribosomal protein L8 (rpl8) used as an internal control of amplified variations. Thermal cycler was started with the hold steps at 95 ℃ for 5 min, followed by 40 cycles of 95 ℃ for 30 s, 56 ℃ for 30 s, and 72 ℃ for 40 s. In this study, 1% agarose gel electrophoresis and melt curve analysis were carried out to assess the specificity of the qRT-PCR products. Relative quantitative expressions of the selected genes with efficiency correction were normalized to rpl8 and determined by the $2^{-\triangle\triangle CT}$ method.

**Table S4.** Sequences of primers used for qRT-PCR validation.

| Gene ID | Gene Name | Gene Description | Primer sequences (from 5′ to 3′) |
|---|---|---|---|
| gene-dio2 | dio2 | deiodinase, iodothyronine, type II | F: GCATAGGCAGTCGCTCATTT<br>R: TGTGGTCTCTCATCCAACCA |
| gene-ttr | ttr | transthyretin (prealbumin, amyloidosis type I) | F: CGGGTGGAGTTTGACACTTT<br>R: GCTCAGAAGGAGAGCCAGTA |
| gene- thrβ | thrβ | thyroid hormone receptor beta | F: TGGGAGATGATACGGGTTGT<br>R: ATAGGTGCCGATCCAATGTC |
| gene- slc5a5 | slc5a5 | solute carrier family 5 (sodium/iodide cotransporter), member 5 | F: GTGGCATGAAGGCTGTAAT<br>R: GATACGGCATCCATTGTTGG |
| gene-rpl8 | rpl8 | ribosomal protein L8 | F: TTGTTGGTGTTGTTGCTGGT<br>R: GGATGCTCAACAGGGTTCAT |

Note: The three genes (dio2, ttr, and thrβ) were the selected DEGs in samples, while slc5a5 is the same genes in all samples but not the DEG. Rpl8 was selected as a housekeeping gene in this study.

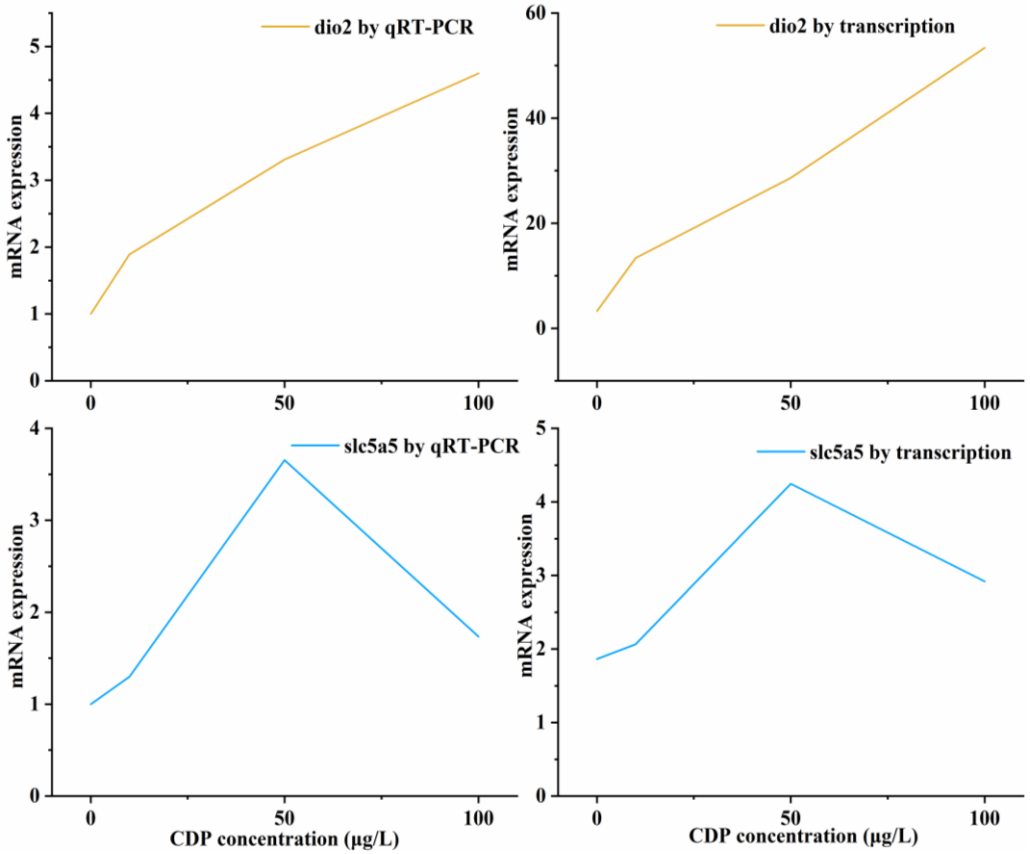


**Figure S3.** Expression analysis of dio2 and slc5a5 via the RNA-seq and qRT-PCR after 28 d exposure.

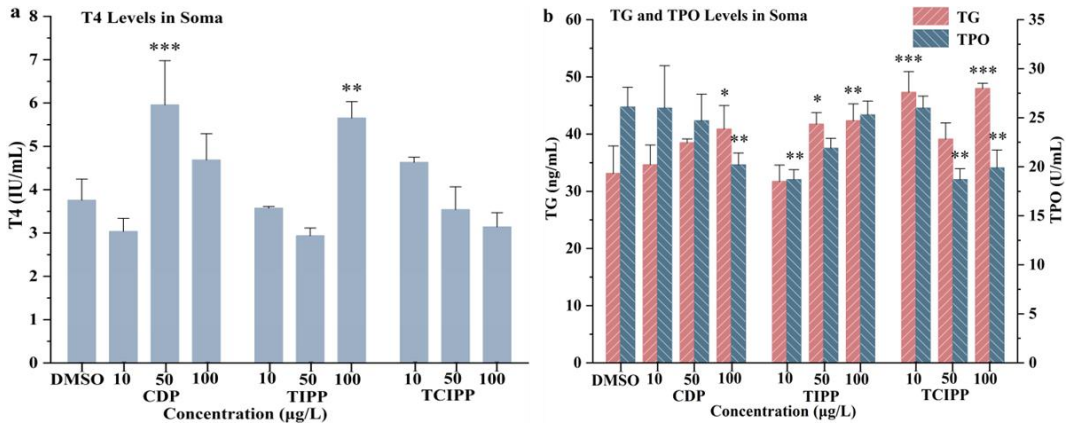


**Figure S4.** Concentrations of T4, TG, and TPO in zebrafish soma exposed to CDP, TIPP, and TCIPP. a represented concentrations of T4 in zebrafish soma exposed to OPEs. Concentrations of TG and TPO in soma after 28 d exposure were measured in Figure S4b. Means ± standard deviation (SD, n = 3), $^{*}$: $p < 0.05$, $^{**}$: $p < 0.01$, $^{***}$: $p < 0.001$.

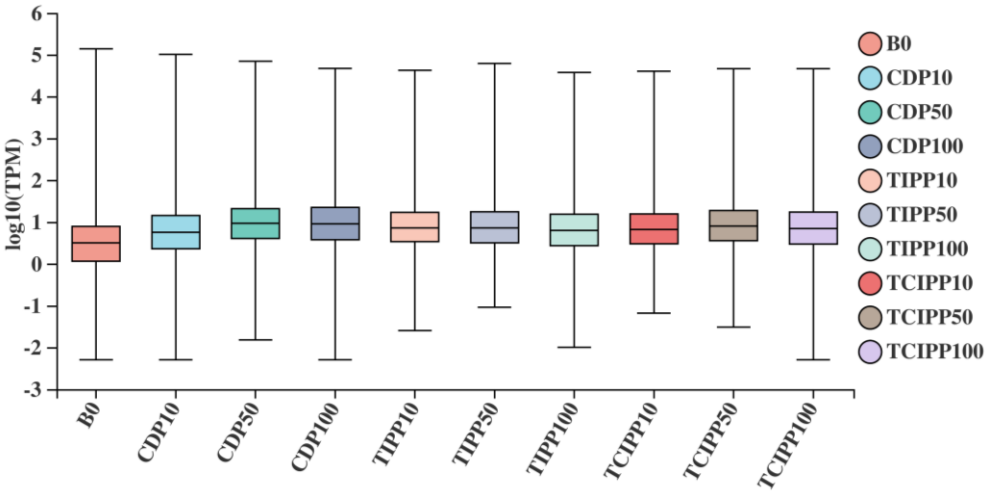


**Figure S5.** Expression of post-transcriptional genes in samples.

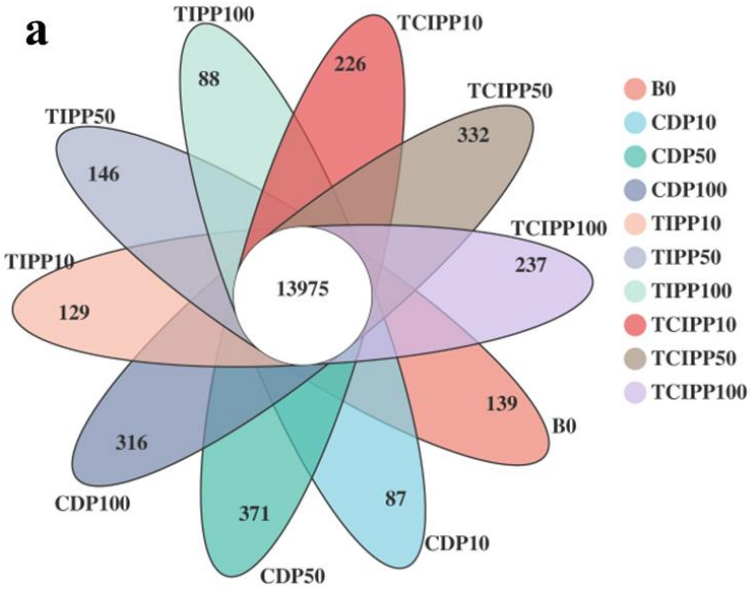

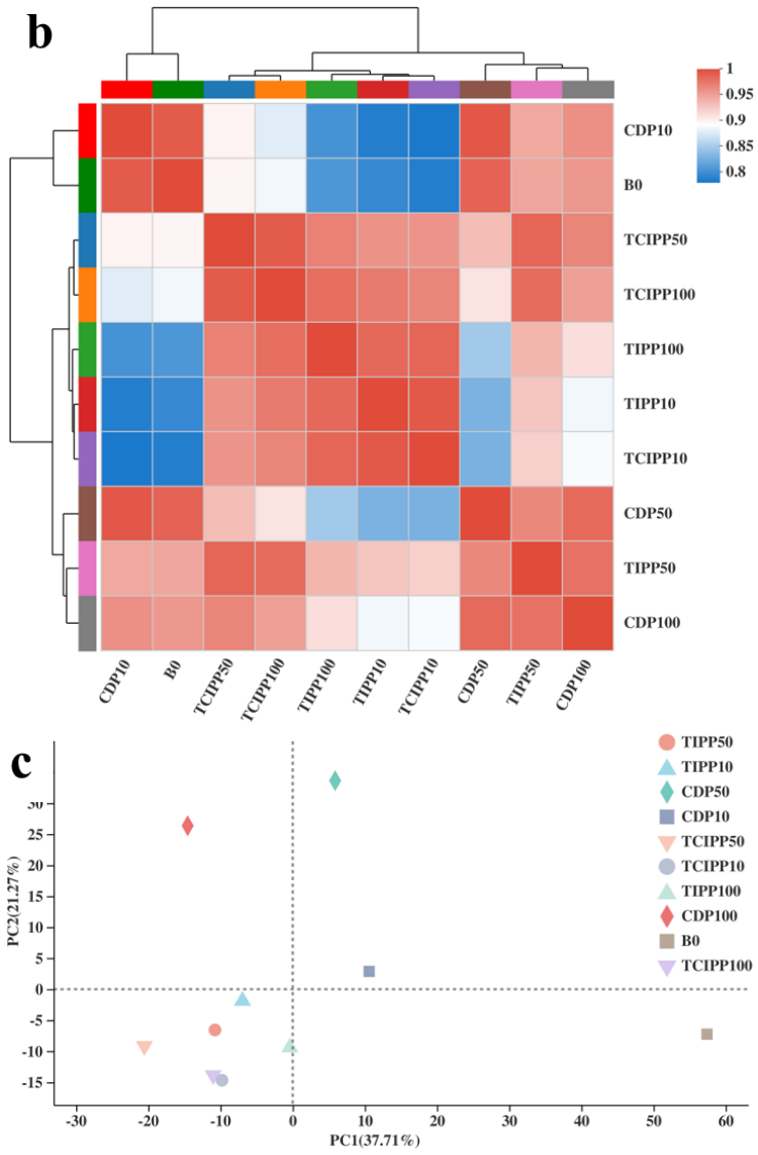


256

257

258 **Figure S6.** Correlation analysis of genes among all samples. a: Venn analysis of all

259 samples; b: Heat map of correlation among OPEs and the controls; c: PCA analysis of

260 three OPEs groups and the controls.

261

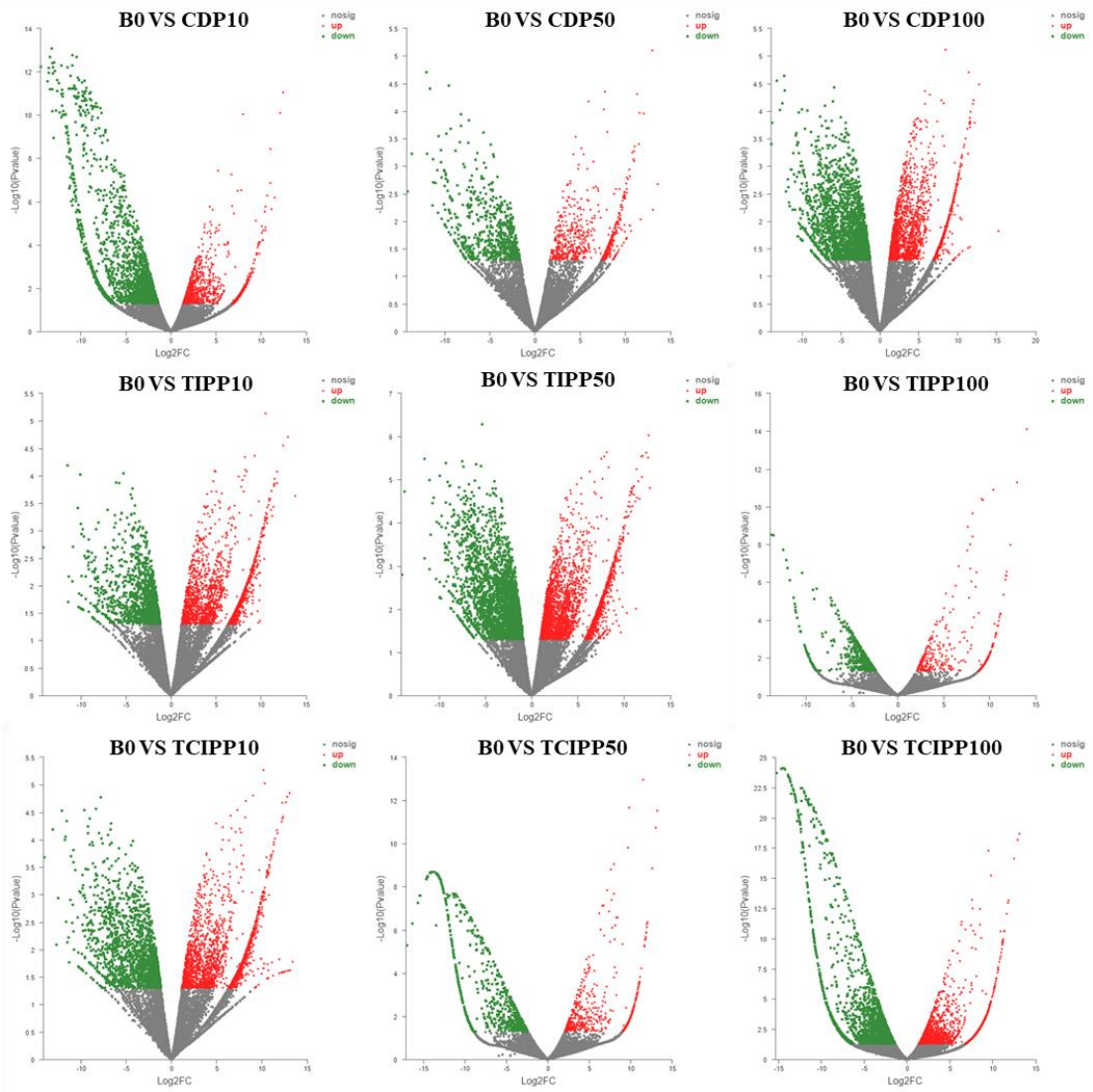


**Figure S7.** Volcano map of DEGs among three OPEs and the blank.

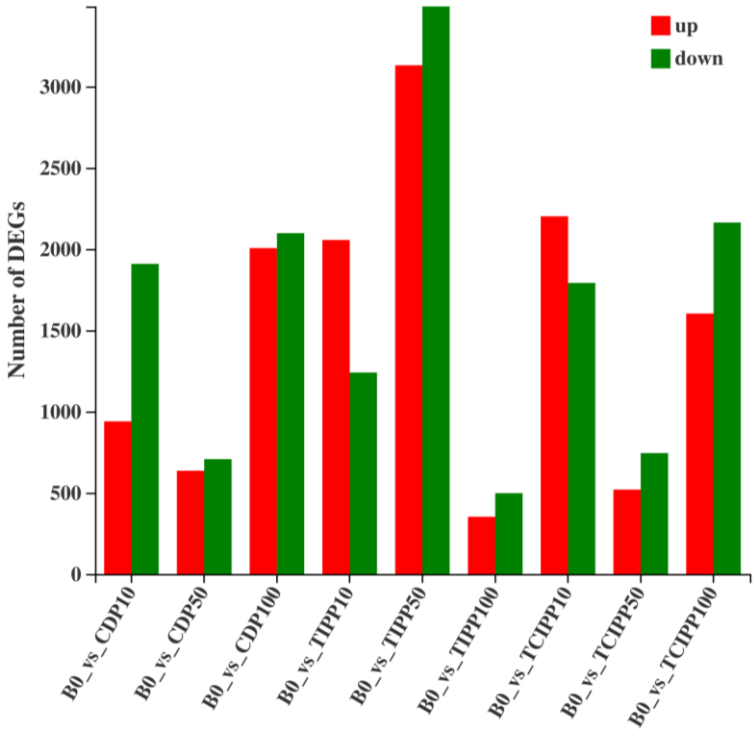


**Figure S8.** Histogram of differential statistics of DEGs among all brain samples.

**Table S5.** Number of DEGs in three OPEs and the control.

| Different Group | Total DEGs | Up | Down |
|---|---|---|---|
| B0_vs_CDP10 | 2847 | 939 | 1908 |
| B0_vs_CDP50 | 1342 | 636 | 706 |
| B0_vs_CDP100 | 4102 | 2005 | 2097 |
| B0_vs_TIPP10 | 3294 | 2055 | 1239 |
| B0_vs_TIPP50 | 6622 | 3130 | 3492 |
| B0_vs_TIPP100 | 849 | 352 | 497 |
| B0_vs_TCIPP10 | 3992 | 2201 | 1791 |
| B0_vs_TCIPP50 | 1263 | 519 | 744 |
| B0_vs_TCIPP100 | 3764 | 1602 | 2162 |

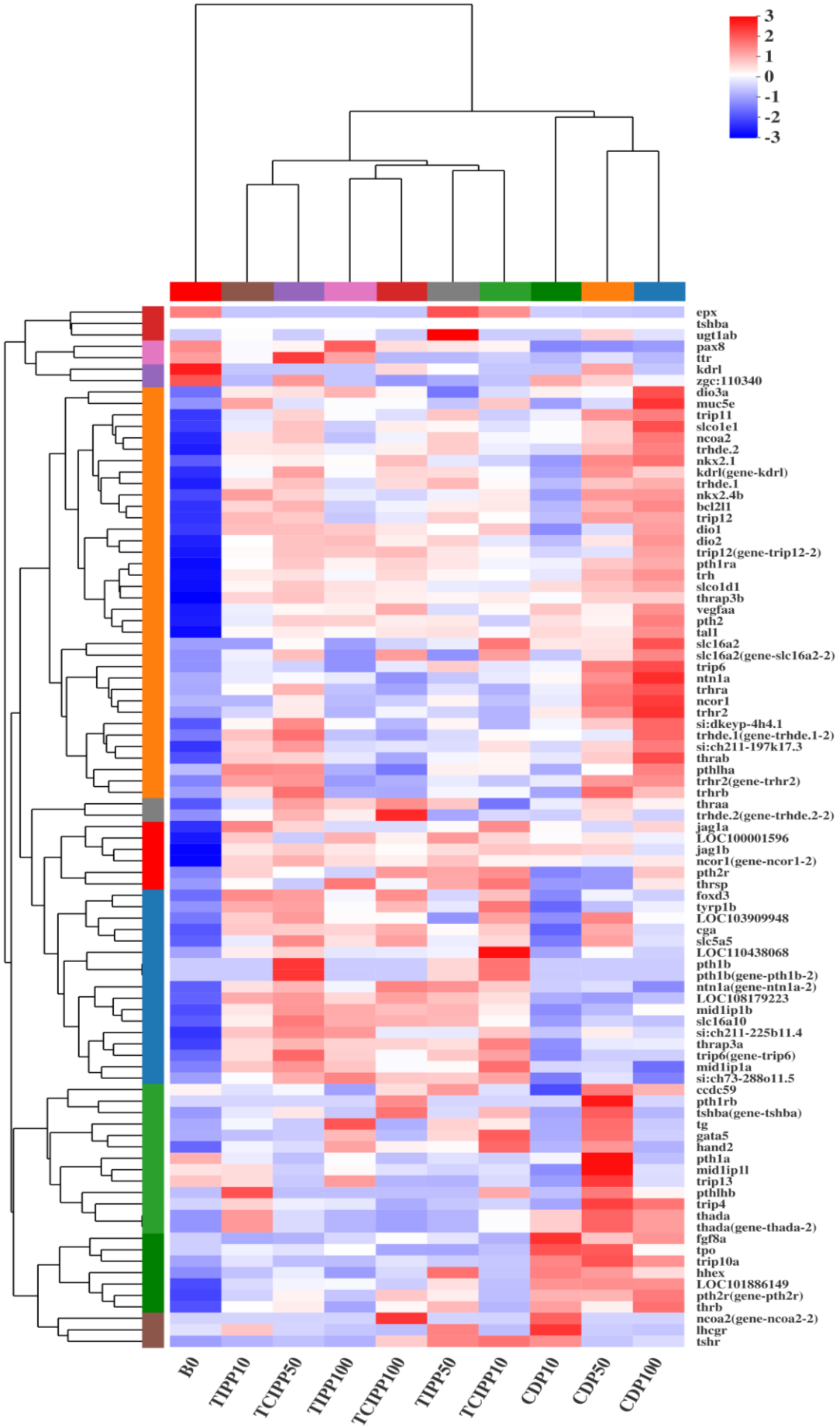
3
2
1
0
-1
-2
-3
epx
tshba
ugt1ab
pax8
ttr
kdrl
zgc:110340
dio3a
muc5e
trip11
slco1e1
ncoa2
trhde.2
nkx2.1
kdrl(gene-kdrl)
trhde.1
nkx2.4b
bcl2l1
trip12
dio1
dio2
trip12(gene-trip12-2)
pth1ra
trh
slco1d1
thrap3b
vegfaa
pth2
tal1
slc16a2
slc16a2(gene-slc16a2-2)
trip6
ntn1a
trhra
ncor1
trhr2
si:dkeyp-4h4.1
trhde.1(gene-trhde.1-2)
si:ch211-197k17.3
thrab
pthlha
trhr2(gene-trhr2)
trhrb
thraa
trhde.2(gene-trhde.2-2)
jag1a
LOC100001596
jag1b
ncor1(gene-ncor1-2)
pth2r
thrsp
foxd3
tyrp1b
LOC103909948
cga
slc5a5
LOC110438068
pth1b
pth1b(gene-pth1b-2)
ntn1a(gene-ntn1a-2)
LOC108179223
mid1ip1b
slc16a10
si:ch211-225b11.4
thrap3a
trip6(gene-trip6)
mid1ip1a
si:ch73-288o11.5
ccdc59
pth1rb
tshba(gene-tshba)
tg
gata5
hand2
pth1a
mid1ip1l
trip13
pthlhb
trip4
thada
thada(gene-thada-2)
fgf8a
tpo
trip10a
hhex
LOC101886149
pth2r(gene-pth2r)
thrb
ncoa2(gene-ncoa2-2)
lhcgr
tshr
B0
TIPP10
TCIPP50
TIPP100
TCIPP100
TIPP50
TCIPP10
CDP10
CDP50
CDP100

**Figure S9.** Hierarchical clustering of 91 thyroid-related genes selected from 47736 genes exposure to CDP, TIPP, and TCIPP in zebrafish brain for all samples. The colors indicated the normalized expression value of the gene in each sample. Red represented overexpressed, while blue represented under-expressed. The left was the tree diagram of genes clustering, the top was the tree diagram of all samples clustering.

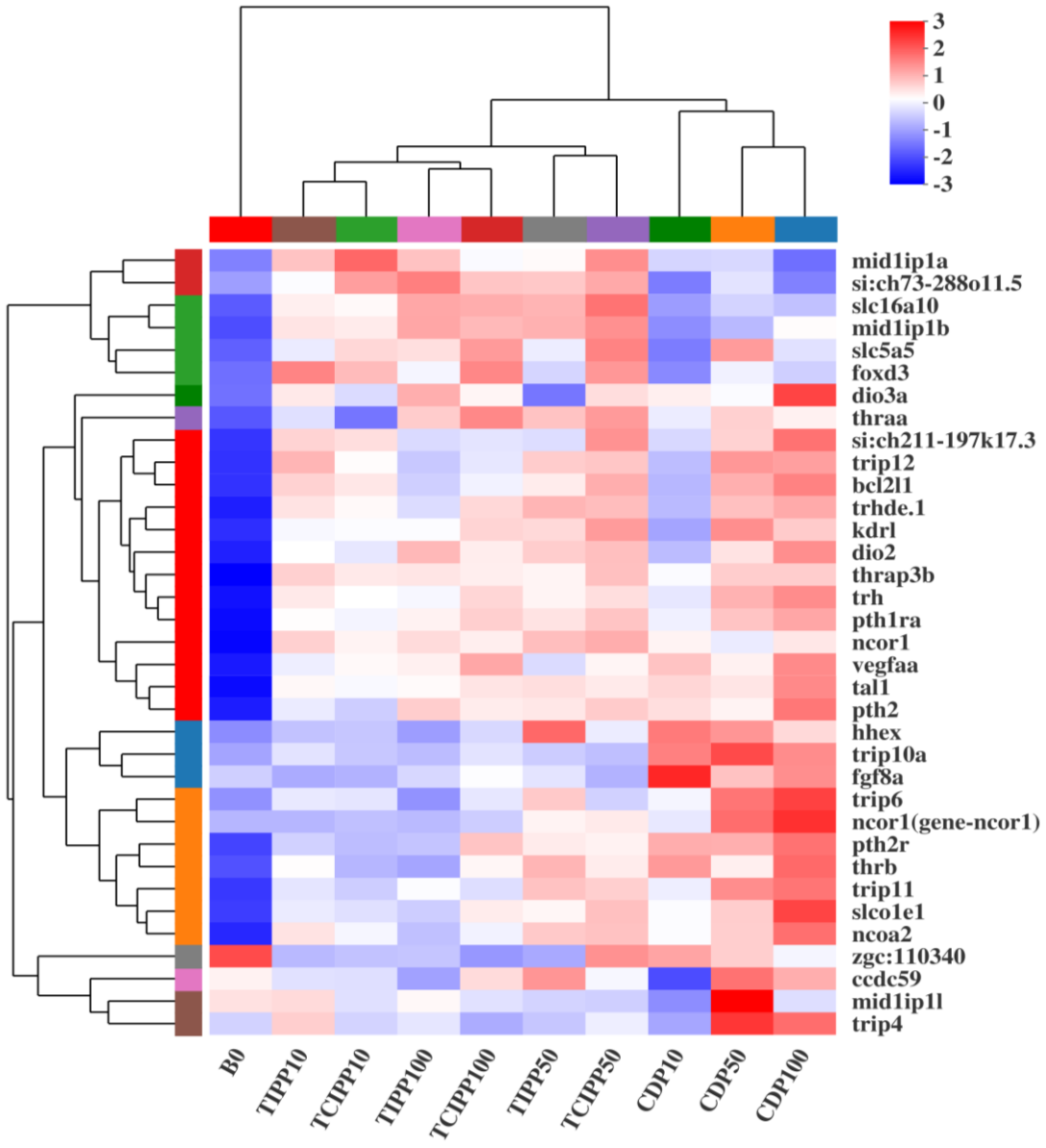


**Figure S10.** Hierarchical clustering of 35 thyroid-related genes selected from 13975 genes exposure to CDP, TIPP, and TCIPP in zebrafish brain for all samples. The colors indicated the normalized expression value of the gene in each sample. Red represented overexpressed, while blue represented under-expressed. The left was the tree diagram of genes clustering, the top was the tree diagram of all samples clustering.

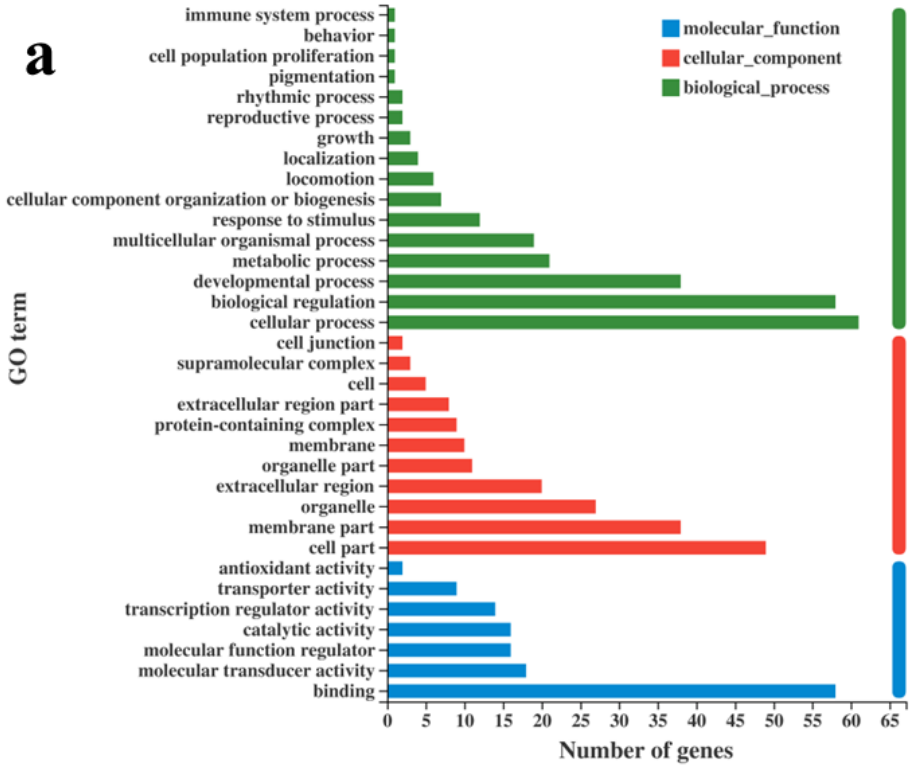
a
molecular_function
cellular_component
biological_process
GO term
immune system process
behavior
cell population proliferation
pigmentation
rhythmic process
reproductive process
growth
localization
locomotion
cellular component organization or biogenesis
response to stimulus
multicellular organismal process
metabolic process
developmental process
biological regulation
cellular process
cell junction
supramolecular complex
cell
extracellular region part
protein-containing complex
membrane
organelle part
extracellular region
organelle
membrane part
cell part
antioxidant activity
transporter activity
transcription regulator activity
catalytic activity
molecular function regulator
molecular transducer activity
binding
0 5 10 15 20 25 30 35 40 45 50 55 60 65
Number of genes

282

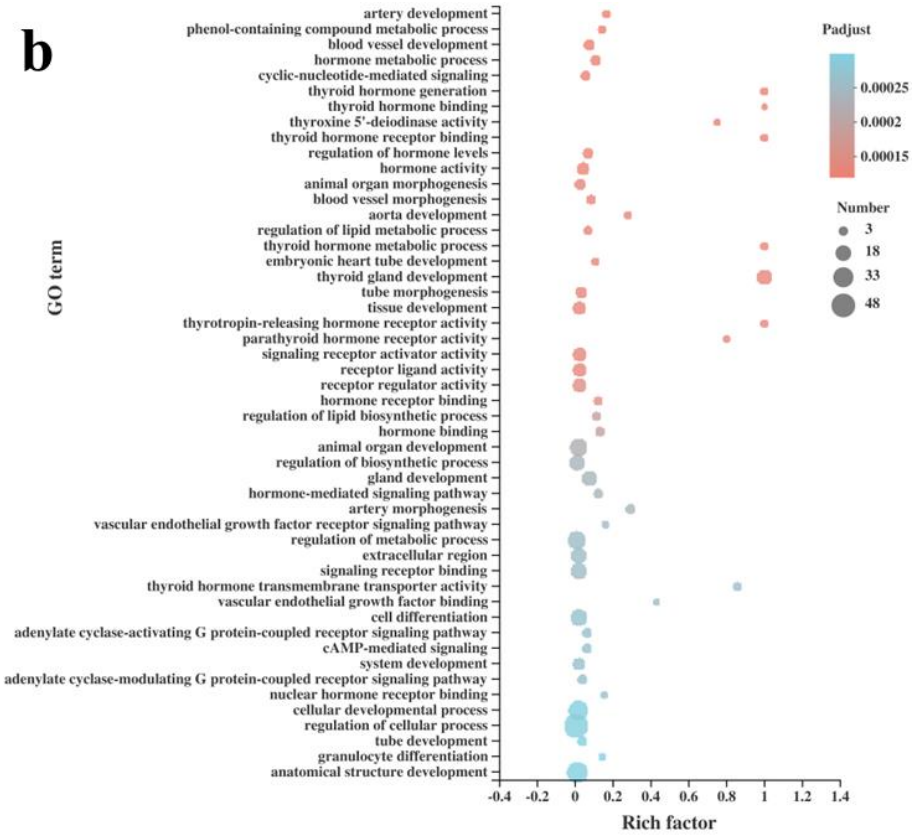
b
GO term
artery development
phenol-containing compound metabolic process
blood vessel development
hormone metabolic process
cyclic-nucleotide-mediated signaling
thyroid hormone generation
thyroid hormone binding
thyroxine 5'-deiodinase activity
thyroid hormone receptor binding
regulation of hormone levels
hormone activity
animal organ morphogenesis
blood vessel morphogenesis
aorta development
regulation of lipid metabolic process
thyroid hormone metabolic process
embryonic heart tube development
thyroid gland development
tube morphogenesis
tissue development
thyrotropin-releasing hormone receptor activity
parathyroid hormone receptor activity
signaling receptor activator activity
receptor ligand activity
receptor regulator activity
hormone receptor binding
regulation of lipid biosynthetic process
hormone binding
animal organ development
regulation of biosynthetic process
gland development
hormone-mediated signaling pathway
artery morphogenesis
vascular endothelial growth factor receptor signaling pathway
regulation of metabolic process
extracellular region
signaling receptor binding
thyroid hormone transmembrane transporter activity
vascular endothelial growth factor binding
cell differentiation
adenylate cyclase-activating G protein-coupled receptor signaling pathway
cAMP-mediated signaling
system development
adenylate cyclase-modulating G protein-coupled receptor signaling pathway
nuclear hormone receptor binding
cellular developmental process
regulation of cellular process
tube development
granulocyte differentiation
anatomical structure development
-0.4 -0.2 0 0.2 0.4 0.6 0.8 1 1.2 1.4
Rich factor
Padjust
0.00025
0.0002
0.00015
Number
3
18
33
48

283

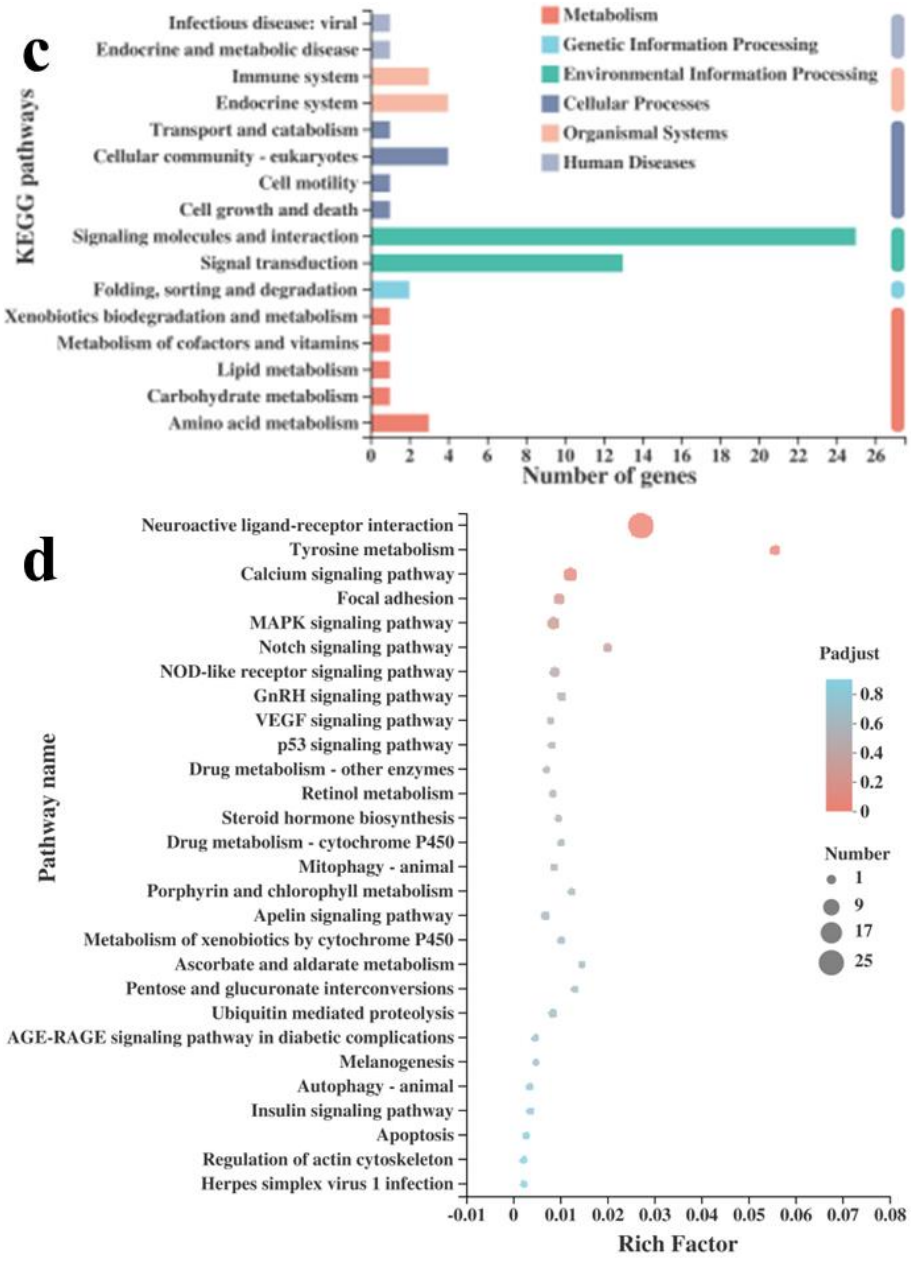


**Figure S11.** Enrichment analysis of signaling pathways obtained by 91 thyroid-related genes based on GO and KEGG database for the all brain samples. Figure S11a was the functional annotation analysis based on GO database, while the functional annotation analysis of KEGG database was showed in Figure S11c. b represented the functional enrichment analysis of GO database for all samples, in which the top 50 GO terms of enrichment were shown (P-adjust < 0.05). d represented the KEGG enrichment analysis of the all KEGG pathways (28) in all samples. Rich factor represented the ratio of the gene number enriched in GO term and the gene annotation number. The more the rich factor was, the more degree of enrichment was. The size of the dot indicated the number of genes in the GO term, and the color of dot was corresponded to the P-adjust ranges.

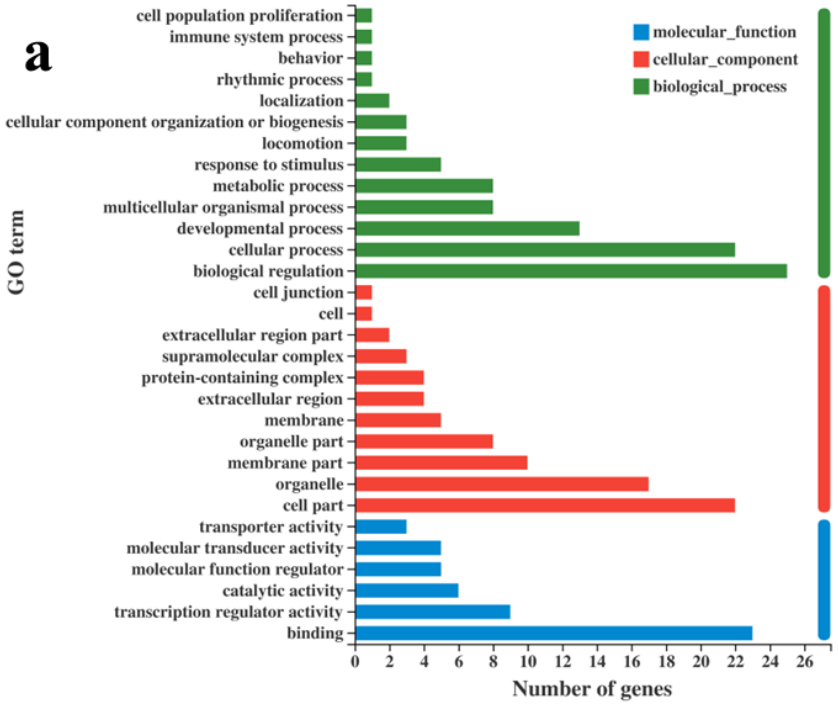
a
molecular_function
cellular_component
biological_process
GO term
cell population proliferation
immune system process
behavior
rhythmic process
localization
cellular component organization or biogenesis
locomotion
response to stimulus
metabolic process
multicellular organismal process
developmental process
cellular process
biological regulation
cell junction
cell
extracellular region part
supramolecular complex
protein-containing complex
extracellular region
membrane
organelle part
membrane part
organelle
cell part
transporter activity
molecular transducer activity
molecular function regulator
catalytic activity
transcription regulator activity
binding
0 2 4 6 8 10 12 14 16 18 20 22 24 26
Number of genes

296

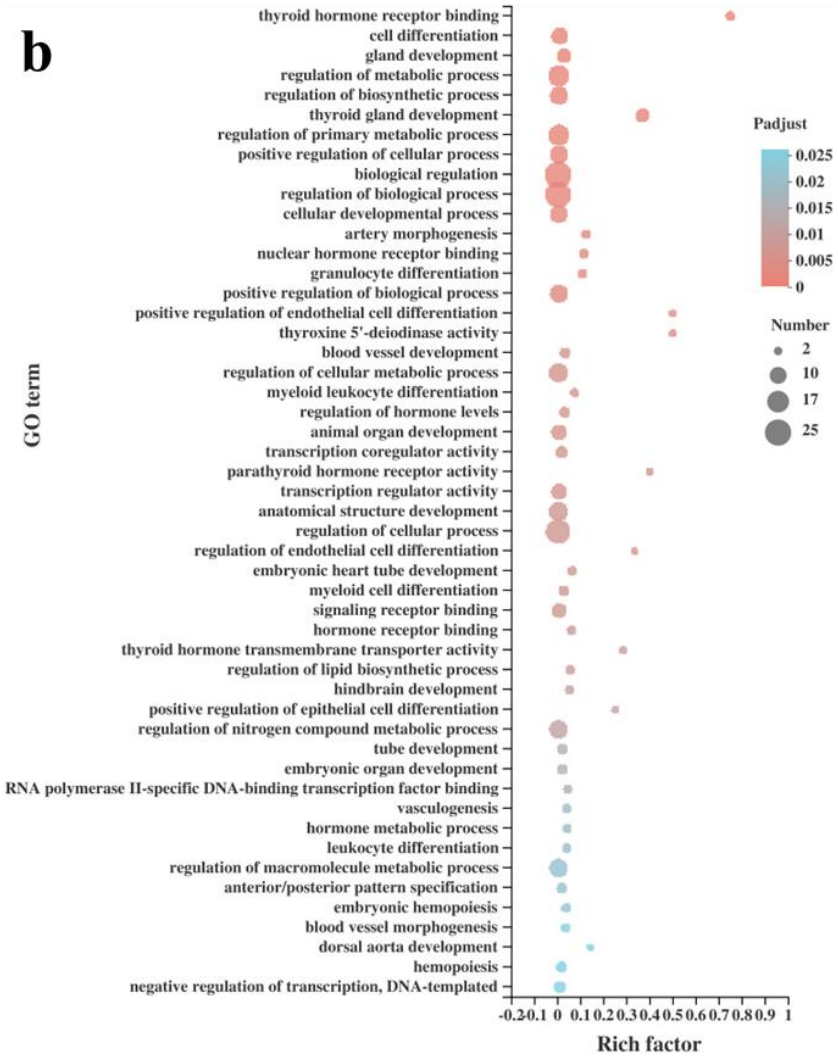
b
GO term
thyroid hormone receptor binding
cell differentiation
gland development
regulation of metabolic process
regulation of biosynthetic process
thyroid gland development
regulation of primary metabolic process
positive regulation of cellular process
biological regulation
regulation of biological process
cellular developmental process
artery morphogenesis
nuclear hormone receptor binding
granulocyte differentiation
positive regulation of biological process
positive regulation of endothelial cell differentiation
thyroxine 5'-deiodinase activity
blood vessel development
regulation of cellular metabolic process
myeloid leukocyte differentiation
regulation of hormone levels
animal organ development
transcription coregulator activity
parathyroid hormone receptor activity
transcription regulator activity
anatomical structure development
regulation of cellular process
regulation of endothelial cell differentiation
embryonic heart tube development
myeloid cell differentiation
signaling receptor binding
hormone receptor binding
thyroid hormone transmembrane transporter activity
regulation of lipid biosynthetic process
hindbrain development
positive regulation of epithelial cell differentiation
regulation of nitrogen compound metabolic process
tube development
embryonic organ development
RNA polymerase II-specific DNA-binding transcription factor binding
vasculogenesis
hormone metabolic process
leukocyte differentiation
regulation of macromolecule metabolic process
anterior/posterior pattern specification
embryonic hemopoiesis
blood vessel morphogenesis
dorsal aorta development
hemopoiesis
negative regulation of transcription, DNA-templated
Padjust
0.025
0.02
0.015
0.01
0.005
0
Number
2
10
17
25
-0.2 -0.1 0 0.1 0.2 0.3 0.4 0.5 0.6 0.7 0.8 0.9 1
Rich factor

297

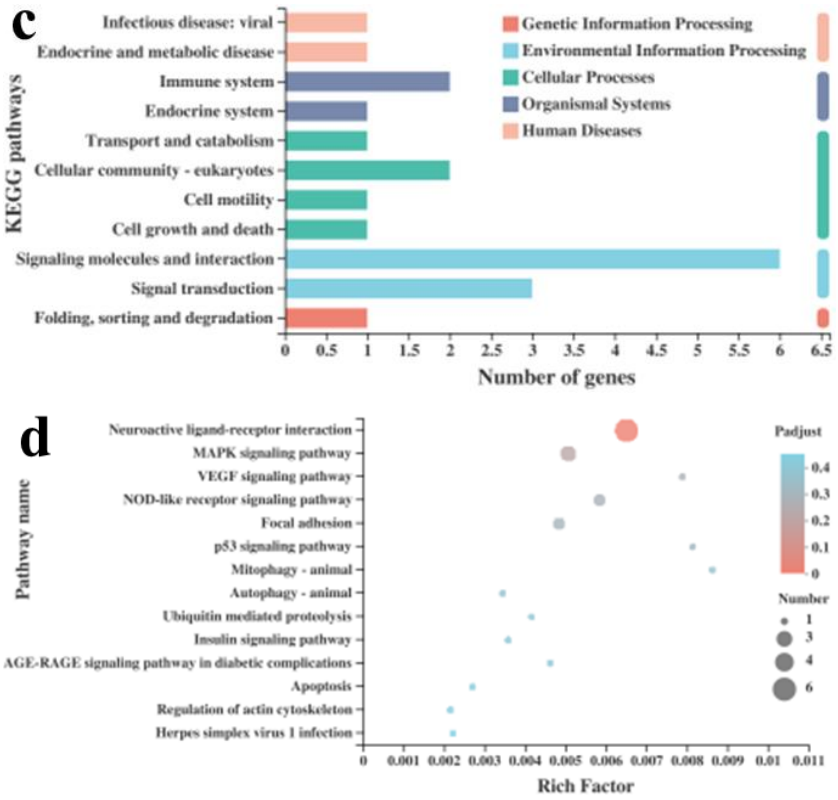


**Figure S12.** Enrichment analysis of signaling pathways obtained by 35 thyroid-related genes selected from 13975 genes based on GO and KEGG database for the all brain samples. Figure S12a was the functional annotation analysis based on GO database, while the functional annotation analysis of KEGG database was showed in Figure S12c. b represented the functional enrichment analysis of GO database for all samples, in which the top 50 GO terms of enrichment were shown (P-adjust < 0.05). d represented the KEGG enrichment analysis of the all KEGG pathways (14) in all samples. Rich factor represented the ratio of the gene number enriched in GO term and the gene annotation number. The more the rich factor was, the more degree of enrichment was. The size of the dot indicated the number of genes in the GO term, and the color of dot was corresponded to the P-adjust ranges.

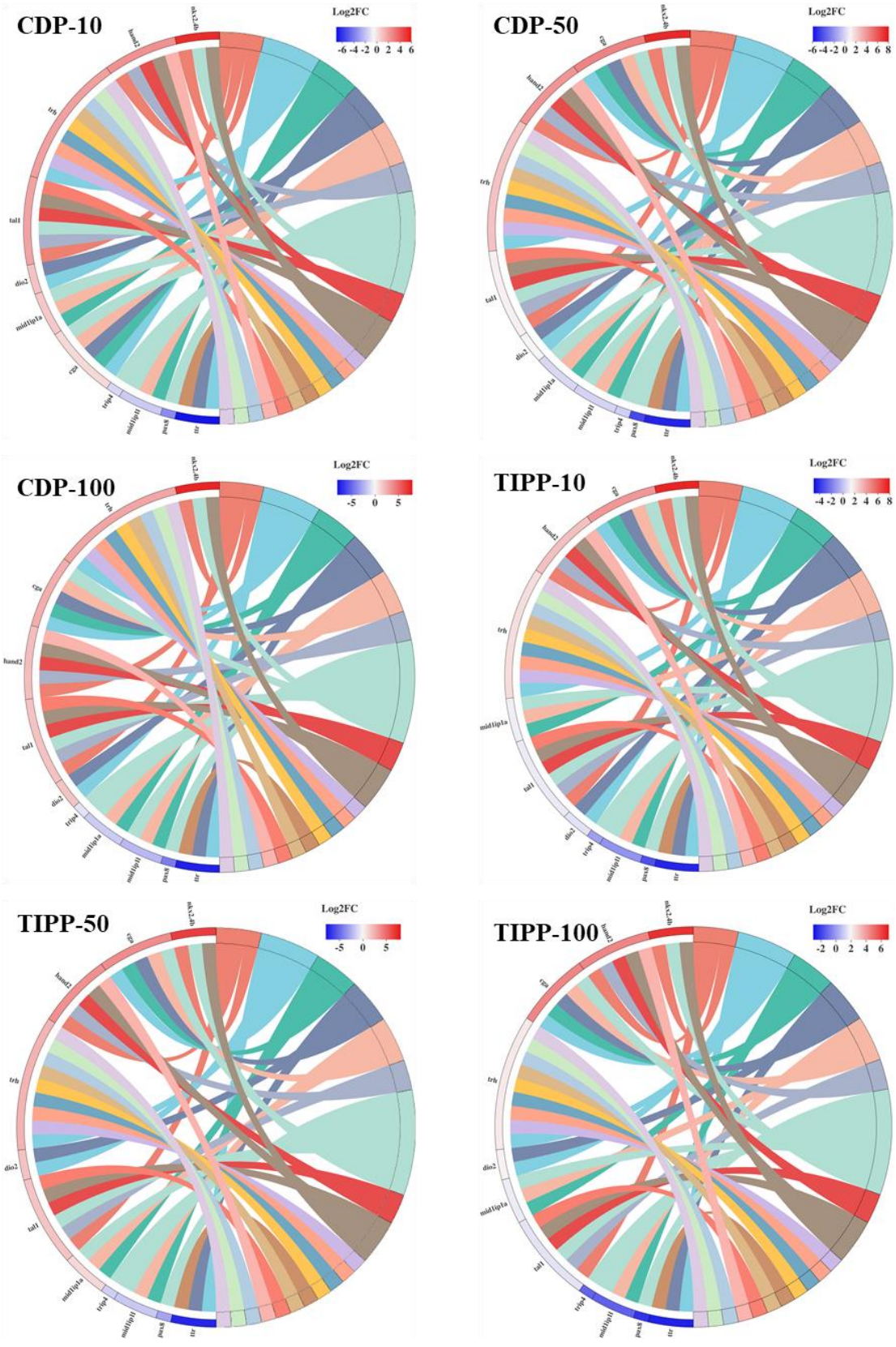
CDP-10
Log2FC
-6 -4 -2 0 2 4 6
CDP-50
Log2FC
-6 -4 -2 0 2 4 6 8
CDP-100
Log2FC
-5 0 5
TIPP-10
Log2FC
-4 -2 0 2 4 6 8
TIPP-50
Log2FC
-5 0 5
TIPP-100
Log2FC
-2 0 2 4 6

312

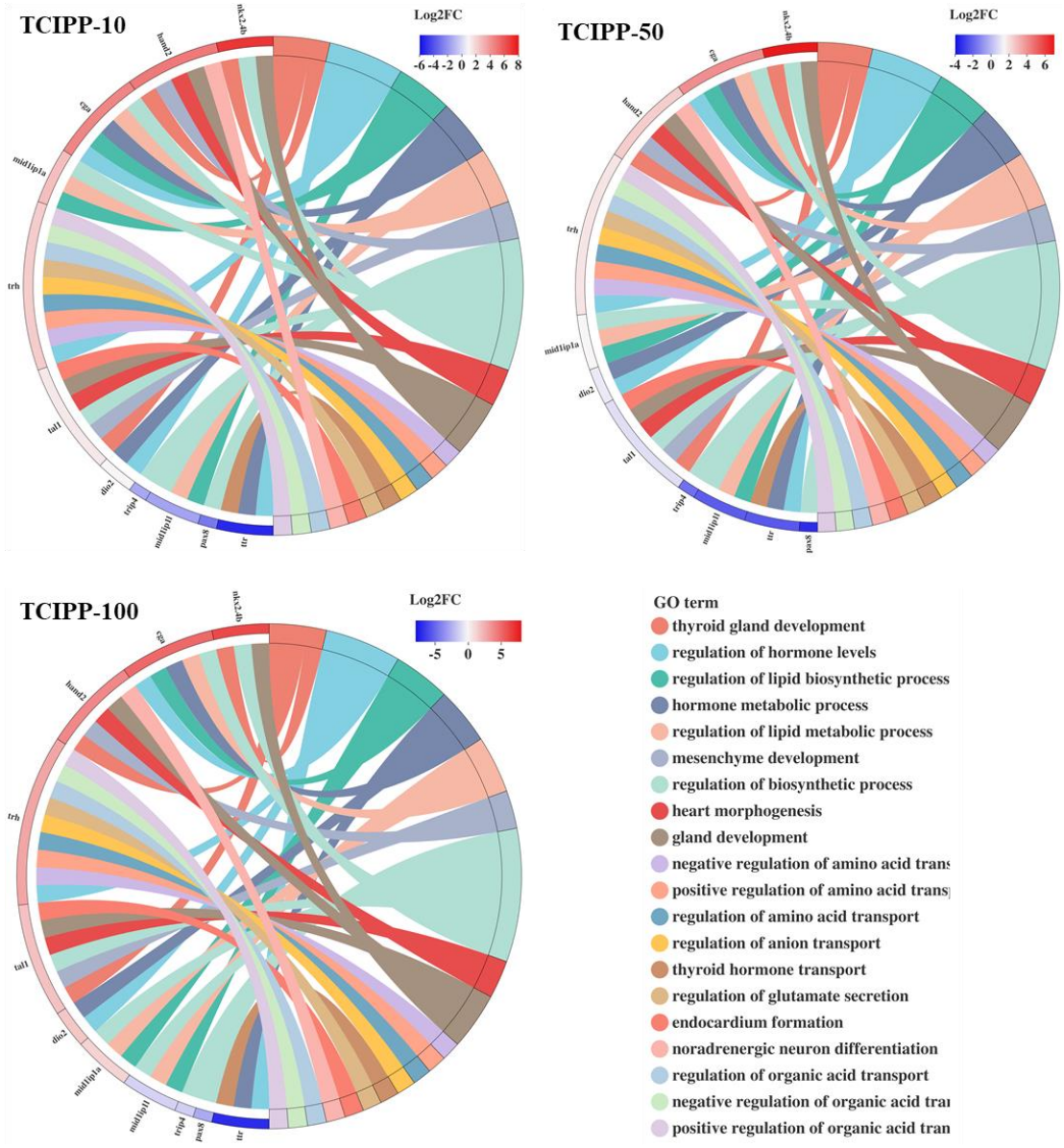


**Figure S13.** Enriched chord diagram of the top 20 GO term enriched by DEGs (24 genes) for all sample exposure to CDP, TIPP, and TCIPP. The left was DEGs, arranged in order of log 2FC from highest to lowest. The right was GO term information enriched by DEGs.

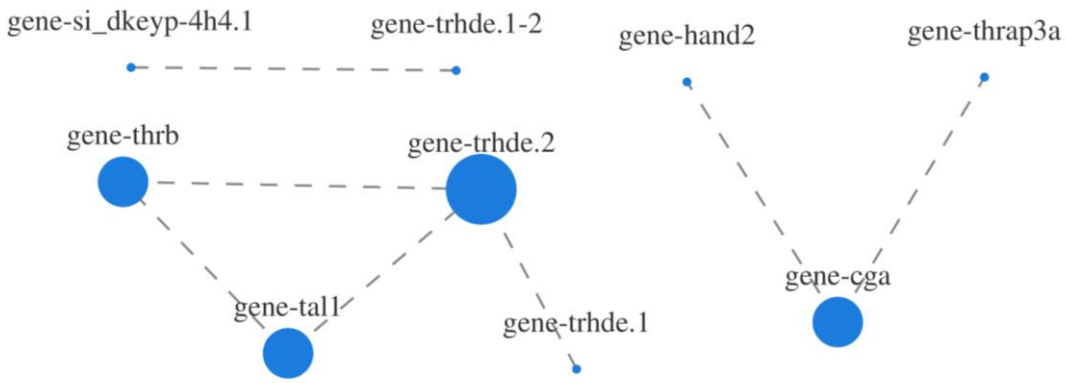


**Figure S14.** Visual presentation of expression correlation among 24 DEGs in zebrafish. Each node represented a gene in the figure, and the line between two nodes showed the correlation of genes expression calculated by the spearman (correlation coefficient > 0.8, P-adjust < 0.05). The figure shown that the larger the node was, the more the number of expression correlation of the gene correlated with other genes was.

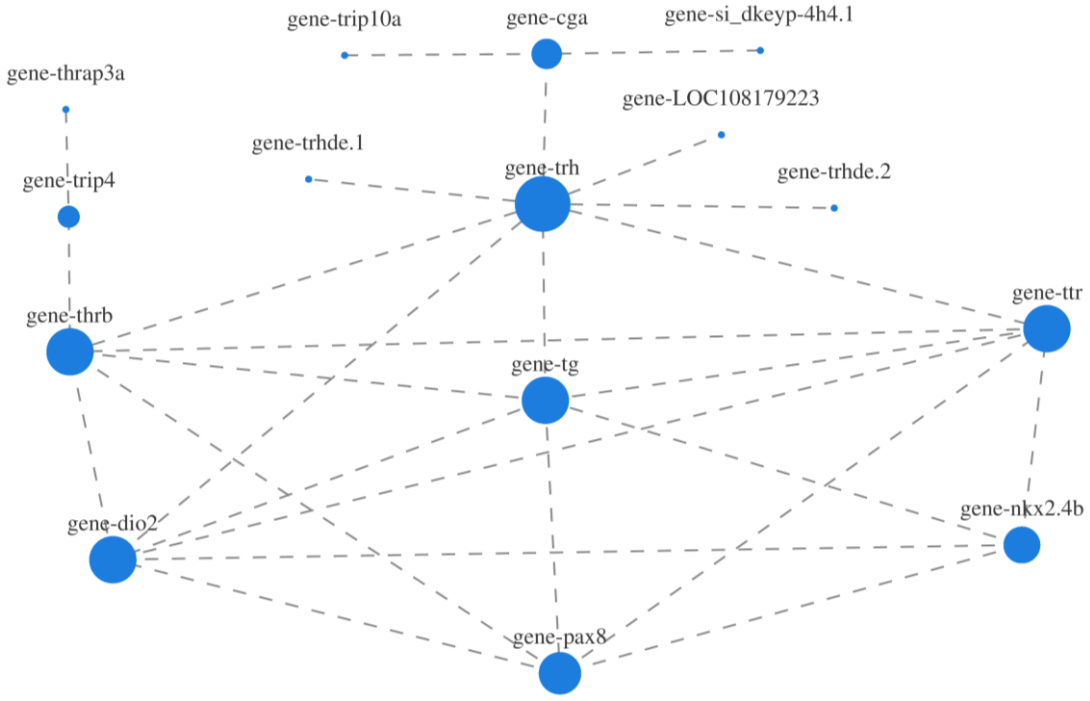


**Figure S15.** Protein interaction network analysis of 24 DEGs in zebrafish. Each node represented a gene in the figure, and the line between two nodes showed the protein interaction. The size of a node was proportional to the connectivity (degree) of the node. The more lines connected to the node, the larger the degree of the node was, and the larger the node will be. It was indicated that the gene played a crucial role in this network.

**Table S6.** Functional enrichment analysis of signaling pathways associated with thyroid system and key events of GO and KEGG databases exposure to OPEs in brain.

| Database | Signal pathway | Thyroid-related genes | P adjust |
|---|---|---|---|
| GO (91 genes) | Thyroid hormone generation | slc5a5, tpo, cga | $1.26 \times 10^{-4}$ |
| | Thyroid hormone binding | slc16a2, ttr | $1.26 \times 10^{-4}$ |
| | Thyroid hormone receptor binding | ncoa2, ncor1 | $1.26 \times 10^{-4}$ |
| | Thyroid hormone metabolic process | slc5a5, dio1, tpo, cga | $1.36 \times 10^{-4}$ |
| | Thyroid gland development | hhex, kdrl, thrαa, thrαb, bcl2l1, tal1, slc16a2, nkx2.4b, ntn1a, vegfaa, fgf8a, hand2, jag1a, jag1b | $1.36 \times 10^{-4}$ |
| | Parathyroid hormone receptor activity | pth2r, pth1ra, pth1rb | $1.36 \times 10^{-4}$ |
| | Thyroid hormone transmembrane transporter activity | slc16a2, slco1d1, muc5e, slc16a10, slco1e1 | $2.52 \times 10^{-4}$ |
| | Response to thyroid hormone | foxd3, tyrp1b | $1.23 \times 10^{-3}$ |
| | Thyroid hormone mediated signaling pathway | thrαa, thrαb | $1.23 \times 10^{-3}$ |
| | Thyroid hormone receptor coactivator activity | ncoa2-2, ncoa2 | $1.23 \times 10^{-3}$ |
| | Thyroid-stimulating hormone receptor activity | tshr, lhcgr | $5.82 \times 10^{-3}$ |
| | Thyroid hormone transport | ttr | 0.12 |
| KEGG (91 genes) | Neuroactive ligand-receptor interaction | thrαa, thrαb, pth2r, thrβ, pth1ra, pth2, trh, pth1b, tshβa, thrβ, trhra, trhr2, pth1a, cga, tshr, pth1rb, trhrb, lhcgr | $2.56 \times 10^{-15}$ |
| | Tyrosine metabolism | tpo, tyrp1b. epx | $1.04 \times 10^{-2}$ |
| | Calcium signaling pathway | trhra, trhr2, trhrb, lhcgr | $5.49 \times 10^{-2}$ |
| | Focal adhesion | kdrl, vegfaa | 0.22 |
| | MAPK signaling pathway | kdrl,vegfaa, fgf8a | 0.25 |
| | NOD-like receptor signaling pathway | trip6, bcl2l1 | 0.41 |
| | GnRH signaling pathway | cga | 0.48 |
| | VEGF signaling pathway | vegfaa | 0.48 |
| | p53 signaling pathway | bcl2l1 | 0.49 |
| | Retinol metabolism | ugt1ab | 0.51 |
| | Steroid hormone biosynthesis | ugt1ab | 0.51 |
| | Ubiquitin mediated proteolysis | trip12 | 0.58 |

| | | | |
|---|---|---|---|
| | AGE-RAGE signaling pathway in diabetic complications | vegfaa | 0.62 |
| | Insulin signaling pathway | trip10a | 0.70 |
| GO (35 genes) | Thyroid hormone receptor binding | ncor1, ncoa2, ncor1-2 | $5.29 \times 10^{-5}$ |
| | Thyroid gland development | hhex, kdrl, thrαa, bcl2l1, tal1, vegfaa, fgf8a | $1.68 \times 10^{-3}$ |
| | Parathyroid hormone receptor activity | pth2r, pth1ra | $6.07 \times 10^{-3}$ |
| | Thyroid hormone transmembrane transporter activity | slc16a10, slco1e1 | $8.67 \times 10^{-3}$ |
| | Response to thyroid hormone | foxd3 | 0.15 |
| | Thyroid hormone mediated signaling pathway | thrαa | 0.15 |
| | Thyroid hormone receptor coactivator activity | ncoa2 | 0.15 |
| | Thyroid hormone generation | slc5a5 | 0.26 |
| | Thyroid hormone metabolic process | slc5a5 | 0.31 |
| KEGG (35 genes) | Neuroactive ligand-receptor interaction | thrαa, pth2r, thrβ, pth1ra, pth2, trh | $8.49 \times 10^{-3}$ |
| | MAPK signaling pathway | kdrl, vegfaa, fgf8a | 0.22 |
| | VEGF signaling pathway | vegfaa | 0.28 |
| | NOD-like receptor signaling pathway | trip6, bcl2l1 | 0.29 |
| | Focal adhesion | kdrl, vegfaa | 0.30 |
| | p53 signaling pathway | bcl2l1 | 0.32 |
| | Mitophagy - animal | bcl2l1 | 0.36 |
| | Autophagy - animal | bcl2l1 | 0.37 |
| | Ubiquitin mediated proteolysis | trip12 | 0.39 |
| | Insulin signaling pathway | trip10a | 0.40 |
| | AGE-RAGE signaling pathway in diabetic complications | vegfaa | 0.40 |
| | Apoptosis | bcl2l1 | 0.42 |
| | Regulation of actin cytoskeleton | fgf8a | 0.43 |
| | Herpes simplex virus 1 infection | bcl2l1 | 0.45 |
| GO (DEGs) | Thyroid gland development | nkx2.4b, tal1, hand2 | $3.42 \times 10^{-3}$ |
| | Regulation of hormone levels | dio2, cga, ttr, trh | 0.012 |
| | Regulation of lipid biosynthetic process | cga, mid1ip1l, mid1ip1a | 0.027 |
| | Hormone metabolic process | dio2, cga, ttr | 0.056 |
| | Regulation of lipid metabolic process | cga, mid1ip1l, mid1ip1a | 0.075 |
| | Thyroid hormone transport | ttr | 0.30 |

| | | | |
|---|---|---|---|
| | Thyroid hormone binding | ttr | 0.60 |
| | Thyroid hormone generation | cga | 0.69 |
| | Thyroid hormone metabolic process | cga | 0.77 |
| KEGG | Neuroactive ligand-receptor interaction | thrb, pth1a, cga, trh | $1.67 \times 10^{-4}$ |
| (DEGs) | Insulin signaling pathway | trip10a | 0.26 |
| | GnRH signaling pathway | cga | 0.28 |
| | Calcium signaling pathway | LOC108179223 | 0.32 |

336

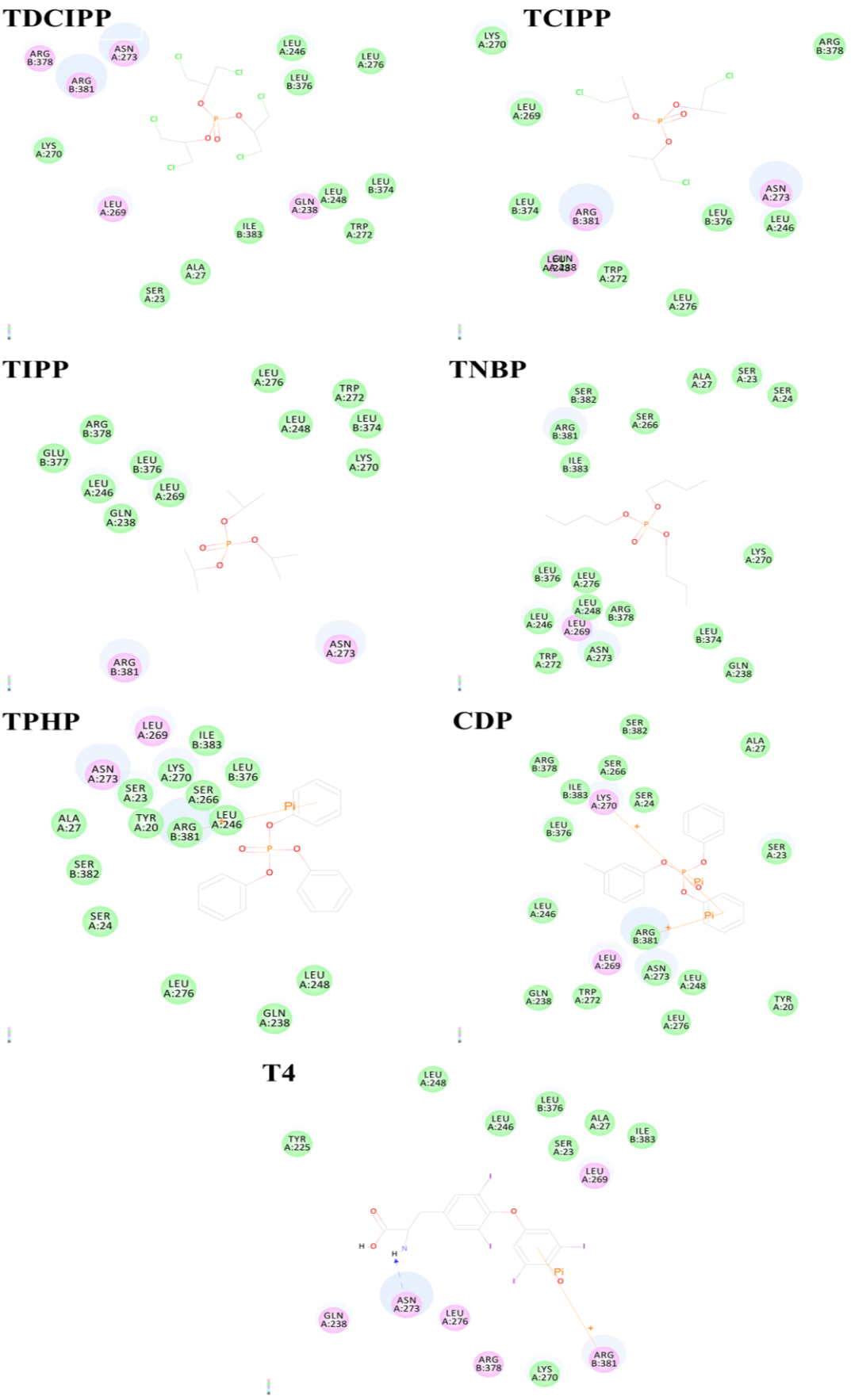


**Figure S16.** Six OPEs and T4 interacted with TBG in molecular docking simulation.

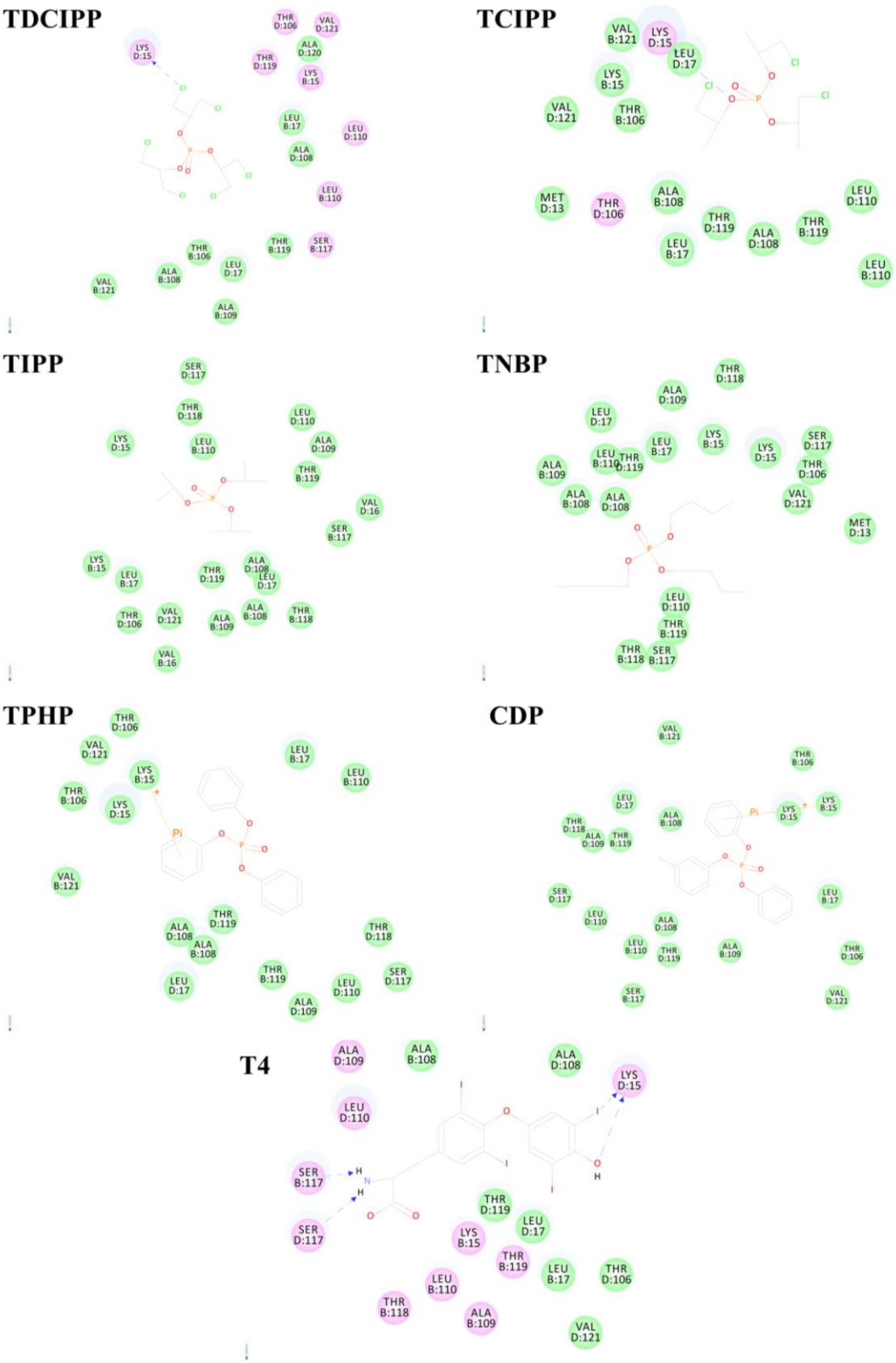


**Figure S17.** Six OPEs and T4 interacted with TTR in molecular docking simulation.

## Literature Cited:


Faria, M., Domingues, R., Paixao, F., Bugalho, M. J., Matos, P., Silva, A. L. 2020. TNFalpha-mediated activation of NF-kappaB downregulates sodium-iodide symporter expression in thyroid cells. *PLoS One 15*(2): e0228794. doi:10.1371/journal.pone.0228794

Gutleb, A. C., Meerts, I. A., Bergsma, J. H., Schriks, M., Murk, A. J. 2005. T-Screen as a tool to identify thyroid hormone receptor active compounds. *Environ Toxicol Pharmacol 19*(2): 231-238. doi:10.1016/j.etap.2004.06.003

Hou, R., Yuan, S., Feng, C., Xu, Y., Rao, K., Wang, Z. 2019. Toxicokinetic patterns, metabolites formation and distribution in various tissues of the Chinese rare minnow (Gobiocypris rarus) exposed to tri(2butoxyethyl) phosphate (TBOEP) and tri-n-butyl phosphate (TNBP). *Science of the Total Environment 668*: 806-814. doi:10.1016/j.scitotenv.2019.03.038

Huang, P., Ren, X., Huang, Z., Yang, X., Hong, W., Zhang, Y., et al. 2014. Serum proteomic analysis reveals potential serum biomarkers for occupational medicamentosa-like dermatitis caused by trichloroethylene. *Toxicol Lett 229*(1): 101-110. doi:10.1016/j.toxlet.2014.05.024

Ji, K., Hong, S., Kho, Y., Choi, K. 2013. Effects of bisphenol s exposure on endocrine functions and reproduction of zebrafish. *Environ Sci Technol 47*(15): 8793-8800. doi:10.1021/es400329t

Kim, S., Jung, J., Lee, I., Jung, D., Youn, H., Choi, k. 2015. Thyroid disruption by triphenyl phosphate an organophosphate flame retardant in zebrafish (Danio rerio) embryos larvae and in GH3 and FRTL-5 cell lines. *Aquatic Toxicology 160*: 188-196. doi:10.1016/j.aquatox.2015.01.016

Kwon, B., Shin, H., Moon, H. B., Ji, K., Kim, K. T. 2016. Effects of tris(2-butoxyethyl) phosphate exposure on endocrine systems and reproduction of zebrafish (Danio rerio). *Environmental Pollution 214*: 568-574. doi:10.1016/j.envpol.2016.04.049

Qiu, W., Chen, B., Greer, J. B., Magnuson, J. T., Xiong, Y., Zhong, H., et al. 2020. Transcriptomic Responses of Bisphenol S Predict Involvement of Immune Function in the Cardiotoxicity of Early Life-Stage Zebrafish (Danio rerio). *Environ Sci Technol 54*(5): 2869-2877. doi:10.1021/acs.est.9b06213

Wang, X. W., Liu, J. F., Yin, Y. G. 2011. Development of an ultra-high-performance liquid chromatography-tandem mass spectrometry method for high throughput determination of organophosphorus flame retardants in environmental water. *J Chromatogr A 1218*(38): 6705-6711. doi:10.1016/j.chroma.2011.07.067

Zhang, Q., Ji, C., Yin, X., Yan, L., Lu, M., Zhao, M. 2016. Thyroid hormone-disrupting activity and ecological risk assessment of phosphorus-containing flame retardants by in vitro, in vivo and in silico approaches. *Environmental Pollution 210*: 27-33. doi:10.1016/j.envpol.2015.11.051

Zhu, Y., Ma, X., Su, G., Yu, L., Letcher, R. J., Hou, J., et al. 2015. Environmentally Relevant Concentrations of the Flame Retardant Tris(1,3-dichloro-2-propyl) Phosphate Inhibit Growth of Female Zebrafish and Decrease Fecundity. *Environmental Science & Technology 49*(24): 14579-14587. doi:10.1021/acs.est.5b03849

Zhu, Y., Su, G., Yang, D., Zhang, Y., Yu, L., Li, Y., et al. 2017. Time-dependent inhibitory effects of Tris(1, 3-dichloro-2-propyl) phosphate on growth and transcription of genes involved in the GH/IGF axis, but not the HPT axis, in female zebrafish. *Environmental Pollution 229*: 470-478. doi:10.1016/j.envpol.2017.06.024